Validation of ligand tetramers for the detection of antigen-specific lymphocytes

Kristin S. Fitzpatrick[1,2], Hanna N. Degefu[3], Katrina Poljakov[1], Madeleine G. Bibby[1], Allison J. Remington[1,4], Tyler G. Searles[3], Matthew D. Gray[1], Jim Boonyaratanakornkit[1], Pamela C. Rosato[3], and Justin J. Taylor[1,5,6]*

[1]Vaccine and Infectious Disease Division, Fred Hutchinson Cancer Center, Seattle, WA, USA
[2]Molecular Medicine and Mechanisms of Disease PhD Program, University of Washington, Seattle, WA, USA
[3]Department of Microbiology and Immunology, Geisel School of Medicine at Dartmouth College, Lebanon, NH, USA
[4]Division of Dermatology, Department of Medicine, University of Washington, Seattle, WA, USA
[5]Department of Immunology, University of Washington, Seattle, WA, USA
[6]Department of Global Health, University of Washington, Seattle, WA, USA
*Contact: jtaylor3@fredhutch.org, @JustinTaylorLab, @JustinTaylorLab@sciencemastodon.com

ABSTRACT

The study of antigen-specific lymphocytes has been a key advancement in immunology the past few decades. The development of multimerized probes containing antigens, peptide:MHC complexes, or other ligands was one innovation allowing the direct study antigen-specific lymphocytes by flow cytometry. While these types of studies are now common and performed by thousands of laboratories, quality control and assessment of probe quality is often minimal. In fact, many of these types of probes are made in-house and protocols vary between labs. While peptide:MHC multimers can often be obtained from commercial sources or core facilities, few such services exist for antigen multimers. To ensure high quality and consistency with ligand probes, we have developed an easy and robust multiplexed approach using commercially available beads able to bind antibodies specific for the ligand of interest. Using this assay, we have sensitively assessed the performance of peptide:MHC and antigen tetramers and find considerable batch-to-batch variability in performance and stability over time. This assay can also reveal common production errors such as miscalculation of antigen concentration. Unexpectedly, probes including the fluorochrome allophycocyanin exhibited more rapid performance decline compared to probes including the fluorochrome R-phycoerythrin when both were stored at 4°C. This performance decline was reduced for most, but not all, batches when antigen tetramers were instead stored at -20°C in 50% glycerol. This work could set the stage for the development of standardized assays for all commonly used ligand probes to limit lab-to-lab technical variation, and experimental failure due to probe underperformance.

INTRODUCTION

Over the past several decades, the use of fluorochrome-conjugated ligands of all types has become a standard approach to detect antigen-specific lymphocytes by flow cytometry. For antigen-specific B cell detection, the most used tools are fluorochrome-conjugated antigen/peptide tetramers, fluorochrome-conjugated virus-like particles as well as other types of fluorochrome-conjugated ligands (For an incomplete cross-section, see (1-232)). Combined, the use of these types of tools has led to important advances in all fields of immunology, the development of experimentally and/or clinically useful antibodies, and as a starting point for rationally designed vaccine antigens.

Throughout the course of a study analyzing antigen-specific B cells by flow cytometry, it is often necessary to produce dozens of antigen probe batches to conduct experiments over the long periods of time research often takes. Even with strict production protocols, this often means that different individuals have produced different batches of antigens using different lots of reagents, or even different reagents all together. Antigens can also undergo storage for different amounts of

time at different temperatures during the various production steps, or multiple freeze/thaw cycles as protocols often neglect to set strict guidelines for every factor that could influence antigen structure. These issues are magnified across fields, where the same antigen could be produced, purified, and stored using completely different protocols. For example, one researcher may produce an antigen using a bacterial system while another used a mammalian system, which could influence glycosylation, folding, or stability of the antigen. Alternatively, production and purification of an antigen may in one case include multiple freeze/thaw cycles while another protocol would not, which could alter the stability of the antigen probe. Another difference can occur after probe production, when one researcher may produce an antigen tetramer fresh for each experiment, whereas a different researcher stores the tetramer for different amounts of time at 4°C or -20°C before use. Despite these sources of variation, there are typically few validation steps to ensure consistent and reproducible antigen probe performance within each experiment. Here, we describe a rapid and robust approach to validate the quality of B cell antigen and MHC tetramers before and/or within each experiment that can be used to authenticate this key resource.

RESULTS

Comparison of murine B cells binding different batches of an antigen tetramer

As an initial assessment, we tested whether different batches of SARS-CoV-2 RBD APC tetramers would bind the same frequency of murine B cells. These different batches were made using the same protocol and either used the same day or stored for up to 42 weeks before use. For this, spleen and lymph nodes were pooled from multiple animals and divided into three technical replicates for each tetramer batch to gauge technical variability (Fig. 1a). Cells were next incubated with SARS-CoV-2 RBD APC tetramers and a control APC-DyLight755 tetramer that allows

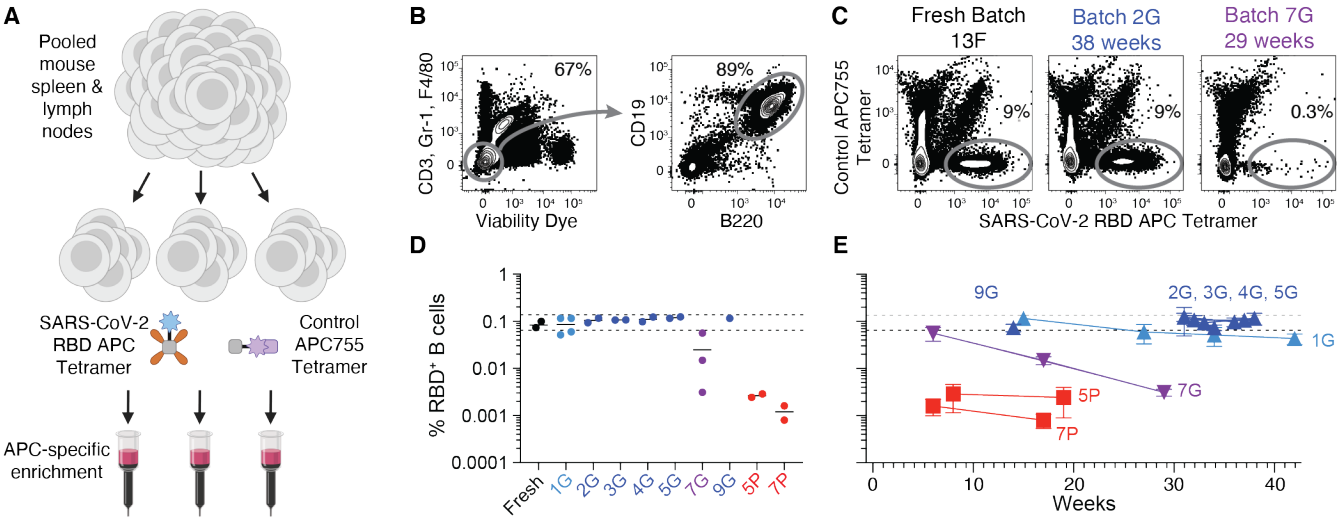

Figure 1. Assessing the frequency of antigen-specific B cells detected using different batches of antigen tetramers. (**A**) Schematic representation of experiments to measure the frequency of antigen-specific murine B cells bound by different batches of SARS-CoV-2 RBD APC tetramers. Spleen and lymph nodes from two to four C57BL/6 mice were pooled and divided evenly into three technical replicates for each tetramer assessed. The samples were next incubated with RBD APC tetramers and a control APC-DyLight755 (APC755) tetramer, followed by magnetic enrichment of tetramer-binding B cells using APC-specific microbeads. The control APC755 tetramers are included to gate out B cells specific for streptavidin-APC. (**B**) Representative flow cytometric gating of live $CD19^+$ $B220^+$ $CD3^-$ $Gr\text{-}1^-$ $F4/80^-$ B cells from an APC-enriched fraction. (**C**) Representative flow cytometric gating of B cells binding to three different batches of RBD APC tetramers, a freshly made batch called 13F, a batch made 38 weeks prior called 2G, and a batch made 29 weeks later called 7G. The % of B cells in the APC-enriched fractions is displayed on the plots. (**D**) Combined data from six experiments showing the frequency of B cells in the starting sample that bound to two freshly made batches of RBD APC tetramers, and 9 batches made previously and stored for various amounts of time at -20°C in 50% glycerol (batches ending with G), or 4°C in 1xDPBS (batches ending with P). Each data point represents the average of three technical replicates and the lines represent means. The dotted lines represent the highest and lowest frequency of RBD-binding B cells obtained using freshly made batches. (**E**) Same data displayed in **D** except displayed versus the amount of time tetramers were stored prior to each use. Data points are displayed along with standard deviation from technical replicates.

for cells binding streptavidin-APC to be excluded from the analysis. Following incubation, tetramer-binding B cells were enriched from the sample using anti-APC microbeads to allow for more robust visualization. Using this approach, ~5% of B cells in the APC-enriched fractions bound to SARS-CoV-2 RBD APC tetramer batches made the day of the experiments, which amounted to ~0.08% of B cells in samples without enrichment (Fig. 1b, c). Likewise, a similar frequency of cells can be found using some SARS-CoV-2 RBD APC tetramers produced as many as 42 weeks earlier when stored at -20°C in 50% glycerol (Fig. 1c, d). Tetramers stored at 4°C in 1xDPBS performed poorly after only a few weeks, as demonstrated by over 30-fold fewer cells binding to tetramers from these batches. Importantly however, storage at -20°C in 50% glycerol did not maintain consistent cell binding of tetramer for all batches (Fig. 1c, d). Analysis of batch 7G revealed that 0.06% of B cells bound this tetramer 6 weeks after production, which was at the lower end of the range found with fresh tetramers (Fig. 1c, d). However, this frequency declined to 0.015% 17 weeks after production, and 0.0031% of cells 29 weeks after production (Fig. 1d). Batch 1G also exhibited a decline in cell binding over time, albeit at a rate slower than that of 7G (Fig. 1d). Together, these data indicate that while storage conditions can help to maintain tetramer performance over time, assessment of these tools is still important to ensure performance.

Bead-based assay to validate tetramer performance

Given the laborious nature of using cell samples to validate tetramer performance, we aimed to develop an easy and robust assay that could be used before, or within every experiment. For this, we expanded upon previously developed bead-based assays (233; 132). For this, eComp Ultra plus compensation beads were incubated with monoclonal antibodies specific for SARS-CoV-2 RBD, positive control antibodies specific for APC, or negative control antibodies specific for PE (Fig. 2a). Following incubation with antibodies, the beads were washed and incubated with tetramer prior to analysis. Using this approach, we found that RBD APC tetramer batch 2G was bound strongly by both anti-APC and the anti-SARS-CoV-2 RBD clone S309 (234), but not anti-PE (Fig. 2b). In contrast, tetramer batch 2P was not bound by S309 but maintained binding by anti-APC (Fig. 2b).

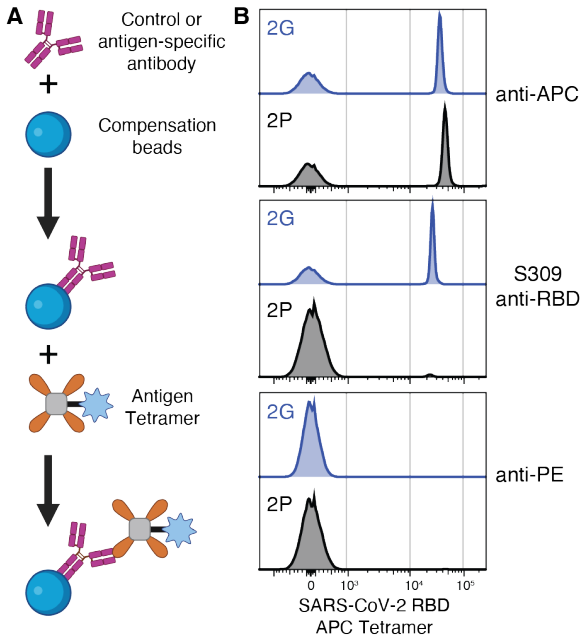

Figure 2. Bead-based approach to assess antigen tetramer performance.
(**A**) Schematic representation of an assay in which compensation beads are loaded with S309 SARS-CoV-2 RBD-specific antibodies, positive control APC-specific antibodies, or negative control anti-PE antibodies prior to incubation with RBD APC tetramers. (**B**) Representative flow cytometric analysis of two different batches of RBD APC tetramers. These batches were produced as a single batch that was split and stored at -20°C in 50% glycerol (2G) or 4°C in 1xDPBS (2P) 36 weeks prior to analysis.

Identification of additional antigen-specific monoclonal antibodies

We next reasoned that assessing tetramer binding by a single antigen-specific antibody clone was not enough to fully validate tetramer performance and expanded the analysis to include additional antibody clones with varied epitope specificities and binding characteristics. For this we used a combination of RBD-specific antibodies identified by others previously (S309, CV30 (235), 204, 208, 211, 215 (182)) as well as antibodies we identified specific for a SARS-CoV-2 spike antigen. For the latter, APC tetramers containing a stabilized spike trimer called S2P (236) were used to identify SARS-CoV-2 spike-specific B cells in APC-enriched PBMCs from convalescent individuals (Fig. 3a). From this screen, six S2P-binding antibodies, named E1, E7, E11, 2B5, 2B8, and 2B11, were identified and used in this study (Fig. 3b). Five of these antibodies bound to RBD with notable differences in off-rate (Fig. 3b,c). The sixth antibody, 2B5, did not bind RBD (Fig. 3b) and was used as a negative control in subsequent RBD

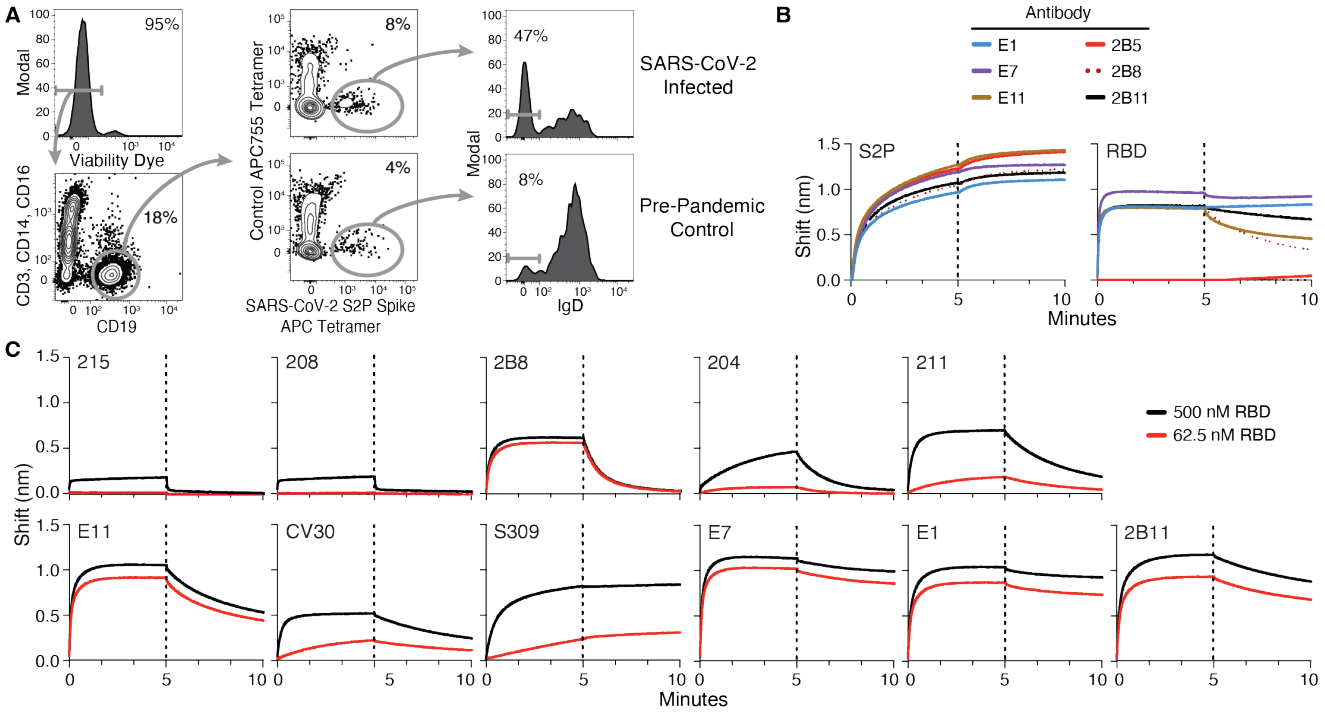

Figure 3. Identification and assessment of antibodies specific for SARS-CoV-2 spike.
(**A**) Representative flow cytometric gating of live CD19^{+} CD3^{-} CD14^{-} CD16^{-} B cells binding SARS-CoV-2 Spike S2P APC tetramers but not APC755 tetramers from PBMCs collected from individuals hospitalized with COVID-19 three-six weeks earlier, and a control sample collected prior to the COVID-19 pandemic. Cells from three COVID-19 patients were concatenated for display. To identify spike-specific antibodies that responded to infection, single S2P-tetramer binding B cells were sorted into individual wells of a 96-well plate and underwent nested RT-PCR followed by Sanger sequencing to identify paired heavy and light chain sequences which were expressed as secreted IgG1. (**B**) Antibodies from six S2P tetramer binding B cells were assessed for binding to S2P or RBD using Bio-Layer Interferometry (BLI). (**C**) BLI assessments of binding of five RBD-binding antibodies from **B** (E1, E7, E11, 2B5, 2B8 & 2B11), and six RBD-specific antibodies from published studies (CV30, S309, 215, 208, 204 & 211) to 62.5 or 500 nM of RBD.

tetramer binding experiments. The mAbs 215 and 208 bound RBD weakly compared to the other antibodies (Fig. 3c).

Multiplexed bead-based tetramer validation assay

To assess the binding of RBD tetramers to multiple RBD-specific and control antibodies, aliquots of beads were co-incubated with an antigen-specific or control antibody as well as an irrelevant fluorochrome-conjugated antibody (Fig. 4a). The fluorochrome-conjugated antibody was included to allow the different antibody-labeled bead populations to be pooled prior to tetramer labeling and distinguished during analysis (Fig. 4b). Using this approach, we included 8 RBD-specific antibodies, anti-APC, anti-PE, and an additional negative control antibody specific for SARS-CoV-2 spike outside of the RBD. After gating on the individual bead populations, we found that different RBD-specific antibodies bound different amounts of RBD-APC tetramers as assessed by gMFI. In general, there was no correlation in the level of tetramer binding of the antibodies bound to beads (Fig. 4c) and the strength of the binding by BLI (Fig. 3c). This disconnect may be the result of avidity gains due to tetramerization of RBD in the bead assay, but not BLI assessment.

When comparing binding in this assay to multiple batches of tetramers, four distinct profiles emerged. The first profile included most of the tetramer batches that were bound by ~0.08% of murine B cells in Figure 1. These tetramers, batches 1G-4G, were bound well by all RBD-specific antibodies and anti-APC (Fig. 4c). The second profile included batches 5P and 7P, which were the tetramer batches bound poorly by murine B cells in Figure 1. Both 5P and 7P exhibited ~100-fold lower binding by all RBD-specific antibodies (Fig. 4c), consistent with poor performance in cell binding assays in Figure 1. The third profile was displayed by batch 7G, which exhibited ~10-fold reduction binding to all RBD-specific antibodies 19

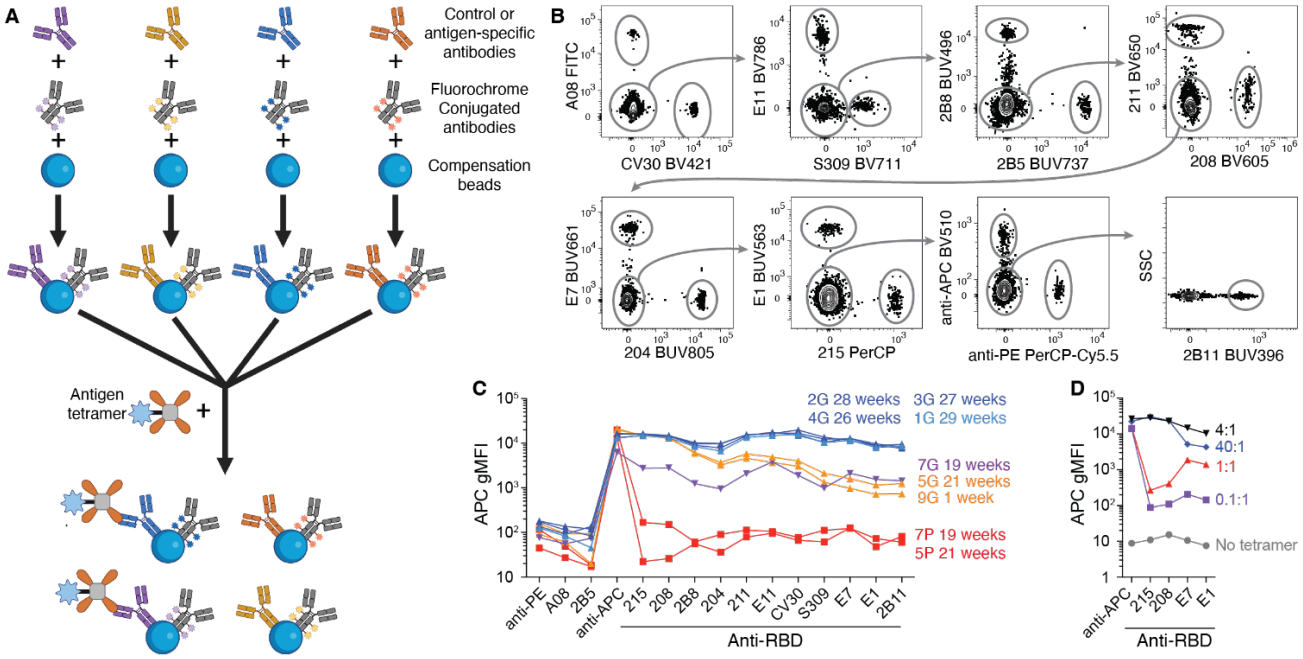

Figure 4. Multiplexed bead-based approach to assess antigen tetramer performance.
(**A**) Schematic representation of an assay in which different populations of compensation beads are loaded with different RBD-specific or control antibodies along with unique fluorochrome-labeled antibodies prior to bead pooling and incubation with RBD APC tetramers. (**B**) Representative flow cytometric gating of fifteen bead populations in a pooled sample. RBD-specific antibodies in the panel are: 215, 208, 2B8, 204, 211, E11, CV30, S309, E7, E1, and 2B11. Negative control antibodies include 2B5, A08 and anti-PE; anti-APC is used as a positive control. (**C**) APC gMFI values of antibody-loaded beads bound to nine different batches of RBD APC tetramers stored for the listed amount of time at -20°C in 50% glycerol (batches ending with G), or 4°C in 1xDPBS (batches ending with P). (**D**) APC gMFI values of antibody-loaded beads bound to batches of antigen probes made by mixing 40, 4, 1, or 0.1 pmole of RBD-biotin to 1 pmole of streptavidin-APC.

weeks after production (Fig. 4c), which is after this batch began performing poorly in enrichment experiments (Fig. 1e).

The final profile was shown by batches 9G and 5G, which exhibited poor binding by some of the RBD-specific mAbs but was bound well by others (Fig. 4c). Interestingly, no reduction in binding was detected for 215 or 208, and only slight reductions in binding for 2B8 and 204 (Fig. 4c). These antibodies also exhibited the poorest binding to RBD when assessed by BLI (Fig. 3c), suggesting that lower affinity antibodies bound batches 9G and 5G well while higher affinity antibodies could not. Upon assessment of the production of batch 9G, it was discovered that the concentration of antigen used to produce this tetramer was 10-fold higher than the 4:1 antigen:streptavidin ratio normally used to produce tetramers. Since the tetramers used in these experiments were not purified prior to use, this means that there were ~36 excess unbound antigen molecules per tetramer molecule contaminating these preparations. Therefore, it seems likely that this unlabeled free antigen was bound by high affinity antibodies, interfering with tetramer binding and detection. Lower affinity antibodies would be expected to be less affected by the presence of free antigen since stable binding is not easily achieved without multimerization. While we did not discover any production errors for batch 5G, we suspect that a similar issue occurred during preparation. Interestingly, batches 5G and 9G were assessed in cellular experiments, and bound ~0.08% of cells, similar to tetramer batches that were performing well (Fig. 1). To confirm that excess free antigen could block binding of high affinity antibodies but not low affinity antibodies, we produced batches in which a 40:1 ratio of RBD-Biotin to streptavidin-APC was compared to a 4:1 ratio. In these experiments, beads loaded with the high affinity antibodies E1 or E7 exhibited reduced binding to the 40:1 batch compared to the 4:1 batch (Fig. 4d). In contrast, beads loaded with the low affinity antibodies 208 or 215 bound similarly to the 40:1 batch and 4:1 batch (Fig. 4d). Together, these results indicate that excess free antigen in tetramer preparations can block the binding of high affinity antibodies, but not binding of lower affinity antibodies expressed by majority of cells in

repertoires without no previous SARS-CoV-2 RBD exposure.

In these experiments we also explored how probes containing fewer than 4 antigen molecules would perform compared to their fully loaded tetramer counterparts. For this we compared probe batches made with RBD-biotin:Streptavidin ratios of 0.1:1 and 1:1, compared to properly made 4:1 RBD tetramers. As expected, the beads loaded with the low affinity antibodies 208 and 215 exhibited ~100-fold loss in binding to the 1:1 batch, which was further reduced at 0.1:1 (Fig. 4d). In contrast, binding by beads loaded with the high affinity antibodies E1 and E7 to the 1:1 batch was only ~10-fold decreased (Fig. 4d). Together, these data highlight the utility of using a bead-based assay to reveal errors in antigen tetramer production resulting in underloaded probes.

Assessment of antigen tetramer stability over time

Using a cocktail of beads bound to different antibodies, we conducted experiments assessing the performance of different batches of tetramers over time under different storage conditions. In total, four batches of RBD APC or RBD PE tetramers were produced, split, and stored at -20°C in 50% glycerol, or stored at 4°C in 1xDPBS. Assessing the APC tetramers revealed that all batches stored at -20°C in 50% glycerol largely maintained stable binding by RBD-specific antibodies over time (Fig. 5). In contrast, RBD APC tetramer batches stored at 4°C in 1xDPBS began to exhibit reduced binding by RBD-specific antibodies as early as 1-3 weeks after production when assessed with CV30, S309 and 2B11 (Fig. 5b). By six weeks after production, most batches stored at 4°C had 5-10-fold reduced binding (Fig. 5b). Antibodies such as 2B8 and E11 also exhibited a decline in binding with slightly slower kinetics (Fig. 5b). These results highlight the importance of using multiple antibodies to assess tetramer performance. Unexpectedly, the batch-to-batch decline in performance varied widely, with batch 2 only exhibiting a moderate loss in binding when stored at 4°C for the 12 weeks assessed. Importantly, the decline in performance was not detected equivalently by each of the RBD-specific antibodies in this experiment.

Antigen tetramer stability with different fluorochromes

We initially predicted that the decline in tetramer performance over time when stored at 4°C in 1xDPBS reflected the stability and half-life of the antigen under these conditions. However, this did not appear to be the case, since RBD PE tetramers were bound well by anti-RBD antibodies for weeks

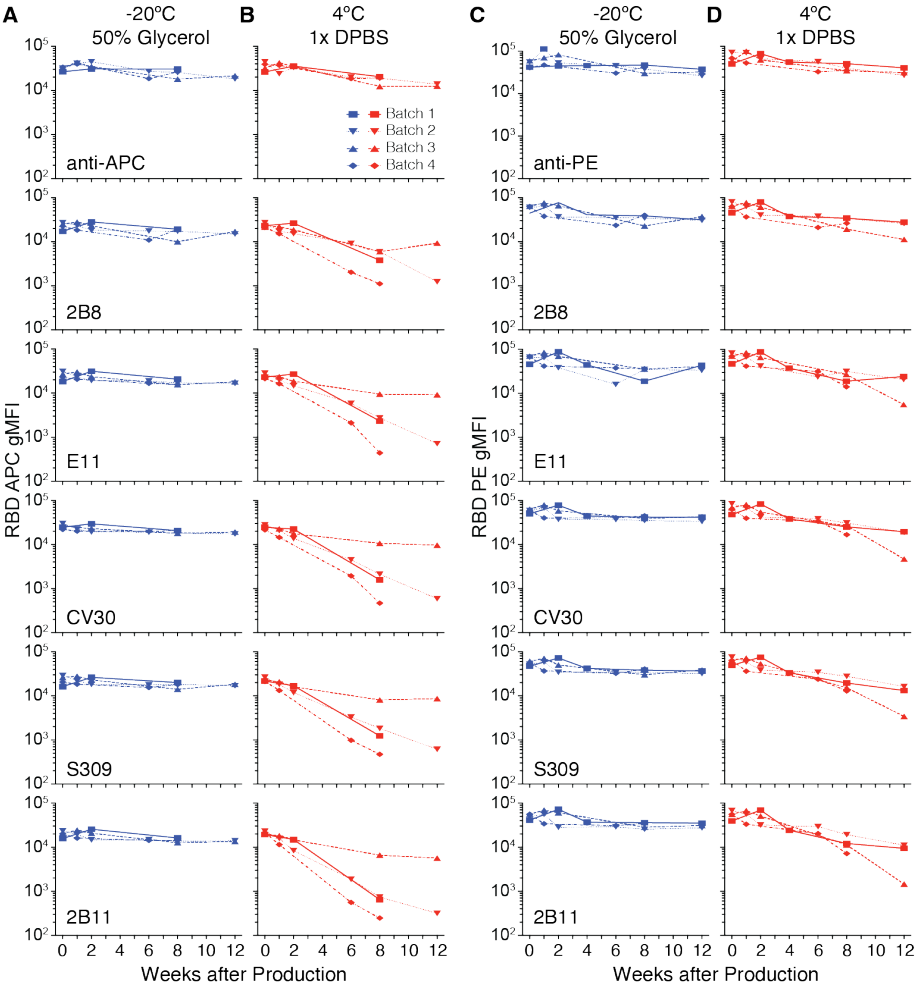

Figure 5. Assessing antigen tetramer performance over time. Combined data from 10 experiments in which four batches of RBD APC tetramers (**A**, **B**) and RBD PE tetramers (**C**, **D**) were assessed using a multiplexed bead assay containing beads loaded with antibodies specific for RBD (2B8, E11, CV30, S309, 2B11) and anti-APC. Each batch of RBD APC and RBD PE tetramers was split in half and stored at -20°C in 50% glycerol (**A**, **C**) or 4°C in 1xDPBS (**B**, **D**).

longer than RBD APC tetramers made at the same time (Fig. 5c-d). Overall, these data suggest that PE-conjugated tetramers are more stable at 4°C compared to APC-conjugated tetramers.

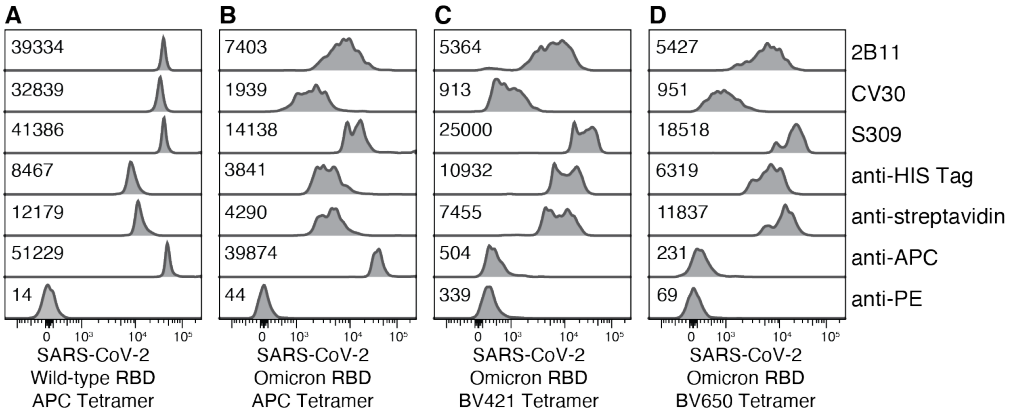

Figure 6. Assessing antigen tetramers utilizing other fluorochromes. Representative data from two experiments in which wild-type RBD APC tetramers, omicron RBD APC tetramers, omicron RBD BV421 tetramers, and omicron RBD BV650 tetramers were assessed for binding to multiplexed beads loaded with anti-RBD (2B11, CV30, S309), anti-HIS tag, anti-streptavidin, anti-APC, or anti-PE. The numbers on the plots represent the gMFI of APC, BV421 or BV650.

Adapting the assay for a wider array of fluorophores

Since APC and PE are not the only fluorochromes used in experiments using ligand tetramer-binding cells, we adapted this assay to include additional positive controls. Since antibodies specific for every possible fluorochrome are not available, we instead produced positive control beads bound to streptavidin-specific antibodies. Compared to APC-specific beads, streptavidin-specific beads bound lower levels of wild-type and omicron RBD APC tetramers (Fig. 6a, b), but at a level sufficient to serve as a positive control for omicron RBD BV421 and BV650 tetramers (Fig. 6c, d). As an additional control in these experiments, we also included beads specific to the 6x-HIS tag included in the RBDs. HIS-specific beads exhibited reduced binding to both wild-type and omicron RBD APC tetramers compared to streptavidin-specific beads, but binding was clearly detectable above the level of binding by the negative control PE-specific beads.

Adapting the assay to test peptide:MHC tetramer stability

The generation of fluorescent multimerized peptide:MHC molecules (237) was a major advance in the detection of antigen-specific T cells. Many peptide:MHC tetramers are commercially available, but these tools are also commonly made by research labs. From both sources these tools can degrade over time to varying degrees. Testing tetramer integrity can be difficult, particularly in the case of human HLA tetramers where clinical samples with a reliable target T cell population may be limiting such as in the case of non-immunodominant epitopes, or cancer neoantigens. Given this, we next assessed whether our multiplexed bead-based assay could be used to test peptide:MHC tetramer stability. For peptide:MHC class I monomers to retain stability, they must include three components: β2m, a heavy chain molecule, and an 8-10 amino acid peptide. A bead-based assay using MHC-specific antibodies has been used to assess tetramer integrity, however this relied on non-commercially available beads and has not been adapted to assess multiple components of the peptide:MHC complex in one reaction (233). To test if our multiplex bead-based assay could be adapted for MHC tetramer, we used an HLA-A*02 PE tetramer loaded with the YLQPRTFLL peptide from SARS-CoV-2 spike ($SARSCov2_{YLQ}$) (238). $SARSCov2_{YLQ}$:HLA-A*02 monomers were made in-house by constructing HLA-A*02 monomer folded with a UV labile peptide as previously described (239-241). UV labile peptide was exchanged for the desired peptide under UV light, then the resulting monomer was tetramerized with streptavidin-PE. We incubated UltraComp beads with antibodies specific for components of the peptide:MHC tetramer complex including heavy chain (HLA-A2 or pan HLA-ABC) human β2m, anti-PE as a positive control and anti-FITC as a negative control (Fig. 7a). As described for antigen tetramers, to enable multiplexing of these bead-antibody conjugates, we included irrelevant fluorochrome-conjugated antibodies to allow the different antibody labeled-bead populations to be pooled prior to $SARSCov2_{YLQ}$ PE tetramer labeling and distinguished during analysis (Fig. 7a). After gating on individual bead populations, we observed high PE gMFI on beads specific for PE, β2m, and HLA-A2 but not negative control beads specific for FITC (Fig. 7b&c). To

confirm this assay can also be used for mouse MHC I tetramers, we incubated H-2K^b APC tetramer loaded with the B8R peptide from vaccinia virus (H2K^b-B8R) (242) with bead-antibody conjugates loaded with antibodies against murine MHC I heavy chain H-2K^b, anti-streptavidin or anti-APC as positive controls, and anti-FITC as a negative control. Consistent with results from the human SARSCov2$_{YLQ}$:HLA-A2 test, we observed strong binding of H2K^b-B8R APC tetramer to H-2K^b-specific beads, streptavidin-specific beads, and APC-specific beads, but not FITC-specific beads (Fig. 7d). Together, indicating this assay can be adapted for the assessment of human and mouse MHC tetramers.

To assess batch-to-batch variability and stability over time, we used the multiplexed-bead assay to compare different batches of HLA-A*02 PE tetramer loaded with the immunodominant peptide GLCTLVAML from Epstein-Barr virus (EBV$_{GLC}$). These different tetramer batches were made using the same batch of UV labile peptide:MHC monomer, but UV peptide exchange and tetramerization were performed 82, 14 or 6 weeks earlier. The results showed a clear difference in the binding ability of tetramer made 82 weeks prior

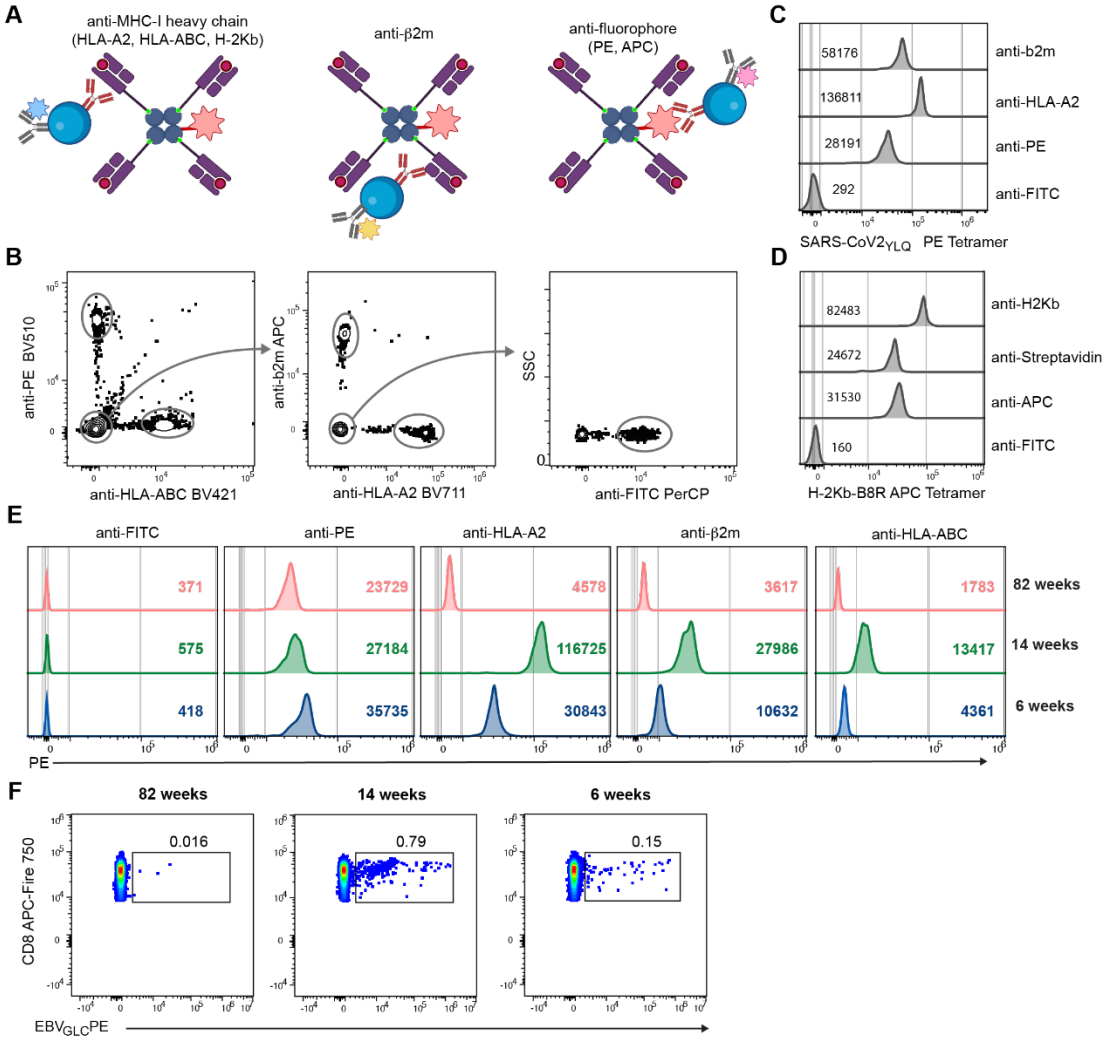

Figure 7. Assessing peptide:MHC tetramers using beads and cells.
(**A**) Schematic representation of peptide:MHC class I tetramer binding to beads loaded with different MHC-specific or fluorophore-specific antibodies along with unique fluorochrome-labeled antibodies to distinguish bead different populations. (**B**) Representative flow cytometric gating of bead populations in pooled sample. (**C, D, E**) Flow cytometry histogram plots showing multiplexed bead staining for human SARSCoV2$_{YLQ}$ PE tetramer (**C**) mouse B8R APC tetramer (**D**) and comparison of three different batches of EBV$_{GLC}$ PE tetramer made 82, 14 and 6 weeks before (E). The numbers on the plots represent gMFI of PE (**C**, **E**) or APC (**D**). (**F**) Flow plots displaying the binding of EBV$_{GLC}$ PE tetramer batches made 82, 14 and 6 weeks before by gated CD3$^+$ CD8$^+$ cells from the same sample of human PBMCs. Data in **B-F** representative of two similar experiments.

compared to more recently made tetramers. Specifically, we observed a reduction in PE gMFI with anti-HLA-A2, -β2m and -HLA-ABC antibodies, indicating a decline in tetramer integrity over time (Fig. 7e). Interestingly, we observed differences in the two recently made tetramers which did not track with time post-production; Tetramer produced 14 weeks prior showed a stronger binding profile than the 6-week-old batch (Fig. 7e). This indicates that in addition to decay over time, there is likely batch-to-batch variability contributing to tetramer integrity.

To test if the difference in binding abilities observed with beads correlates with CD8+ T cell binding ability, we stained a sample of PBMCs from an EBV+ donor with the different batches of EBV_{GLC}-PE tetramer. Similar to the bead-based assay, the tetramer batch made 82 weeks prior exhibited poor performance with a very low frequency of EBV-specific T cells detected. Additionally, while the 6- and 14-week-old batches showed overall improved binding in cell-based assays, the 14-week-old batch had a brighter, more distinct population of tetramer-specific T cells compared to the 6-week-old batch, supporting the observed profile in the bead-based assay (Fig. 7f). This difference may indicate an error in tetramer production with the 6-week-old batch resulting in poor binding ability. Together, these data demonstrate the feasibility of the multiplexed-bead-based assay to test the performance of peptide:MHC tetramers.

DISCUSSION

Here, we have developed an easy and robust assay for assessing the performance of antigen tetramers with the goal of minimizing technical variability and preventing failed experiments due to unreliable and suboptimal tools. The assay utilizes commercially available beads typically used to generate single color controls for compensation bound to monoclonal antibodies specific for the antigen in the tetramer, or MHC complex components, and control antibodies specific for the fluorochrome or streptavidin in the tetramer. By co-labeling the beads with different fluorochrome-labeled antibodies, different populations of beads can be multiplexed into a single tube and each population identified during analysis. This allows for multiple antigen-specific and control antibodies to be utilized in this assay, allowing for coverage of a wide range of binding modalities, epitopes, and in the case of MHC tetramers, components of the peptide:MHC complex. Together, this assay allowed us to detect both improperly produced tetramers, as well as tetramers that performed poorly over time.

Moving forward an assay such as we have described could be standardized to help minimize lab-to-lab differences in reagent quality and ensure reproducibility in similar experiments. Large research consortiums would be well suited to standardize the antibody screening panels for commonly used antigens, as well as controls for normalization of data generated on different flow cytometers by different researchers. Reagent supply companies could also aid this effort by producing antibody-binding beads preloaded with fluorochromes and/or pre-made cocktails targeting commonly used antigens or peptide:MHC components as opposed to the versions we produced in house.

One limitation of the described assay is that it relies upon the availability of previously characterized monoclonal antibodies specific for the antigen of interest. For newly developed or understudied antigens, these may not be readily available. However, given that antibody cloning is often an early step for tetramer validation, we would encourage researchers to utilize these cloned antibodies to assess future tetramer batches to ensure consistency with early studies. Alternatively, it may also be possible to assess tetramer performance using polyclonal antigen-specific antibodies purified from serum.

For MHC tetramer validation, we expanded on a published bead-based assay previously used to assess tetramer performance, but which has not been widely adapted (233). Our use of commercially available beads and multiplexing provides a fast and cost-effective method which may facilitate more widespread adoption of such assays for MHC tetramer validation in the future. While we focused here on MHC I tetramers, the same approaches could be adapted to test MHC II tetramer integrity using commercially available antibodies against human (HLA-DQ, -DR, and -DP) and mouse MHC II (I-A and I-E). While not tested here, antibodies specific for specific peptide:MHC combinations, which can be generated by isolating B cells specific for peptide:MHC (89), may prove even more reliable in testing peptide:MHC tetramer integrity and would enable further multiplexing to test many different tetramers in one reaction.

MATERIALS AND METHODS

Animals

Six- to 14-week-old C57BL/6 male and female mice were purchased from the Jackson Laboratory (Bar Harbor, ME) and maintained in a specific pathogen-free facility in accordance with Fred Hutchinson Cancer Center Institutional Animal Care and Use Committee approval and National Institutes of Health guidelines.

Antigen Tetramers

Biotinylated wild-type RBD and biotinylated omicron RBD was purchased from Sinobiological, or produced and purified in house using the following protocol. The sequence encoding wild-type RBD was cloned into a pTT3 expression vector flanked by an N-terminal TPA signal sequence for protein secretion and a C-terminal 6x histidine-AviTag for purification and subsequent *in vitro* biotin labeling. Briefly, HEK293E cells were transfected at a density of 10^6 cells/mL using 0.5 mg/mL of pTT3-RBD-HISAVI DNA and 2 mg/mL filter sterilized pH 7.0 Polyethylenimine (PEI) MAX (40,000 MW, Polysciences). Six days later, cells and cellular debris were removed by centrifugation at 4,000 × g for 5 minutes followed by filtration through a 0.22 µm Nalgene rapid-flow filter (ThermoFisher Scientific). Clarified supernatant was incubated with His60 Ni-Superflow resin (Takara Bio) overnight at 4°C followed by extensive washing with 0.15 M NaCl, 20 mM Tris, 10mM imidazole (pH 8.0). Antigen was eluted using 250 mM imidazole, 0.3 M NaCl and 20 mM Tris (pH 8.0). Purified protein was concentrated and buffer exchanged into 1xDPBS using a 10kDa MWCO Amicon Ultra-15 centrifugal filter (Millipore Sigma), aliquoted, and frozen in liquid nitrogen and stored at −20°C.

Aliquots of RBD-HISAVI protein were biotinylated *in vitro* using the BirA500:BirA biotin-protein ligase standard reaction kit (Avidity) according to the manufacturer's protocol. After 2 hours incubation at room temperature, unconjugated "free" biotin was removed from RBD by extensive buffer exchanges using a 10kDa MWCO Amicon Ultra-15 centrifugal filter. Concentrated biotinylated protein was collected from the filter and ~0.1 mg aliquots were stored at −20°C.

To confirm the average number of biotin molecules bound to each antigen molecule, streptavidin-PE (PJRS25, ProZyme) was mixed with antigen in increasing ratio and incubated at room temperature for 30 minutes. Mixtures were run on an SDS-PAGE gel (Bio-Rad Laboratories) and transferred to nitrocellulose prior to incubation with streptavidin-Alexa Fluor 680 (ThermoFisher Scientific) diluted in 1x DPBS containing 0.2% Tween-20 (Millipore Sigma). The antigen:streptavidin ratio at which there was a small excess of biotinylated antigen available for streptavidin-Alexa Fluor 680 to bind was the ratio used to make tetramers with streptavidin-PE, streptavidin-APC (PJ27S, ProZyme), streptavidin-BV421 (BD Biosciences), or streptavidin-BV650 (BD Biosciences) for experiments. The molar concentration of each tetramer was calculated by measuring the absorbance of APC, BV421 or BV650 using a NanoDrop Spectrophotometer (ThermoFisher Scientific). Tetramers were stored at 0.1-1 µM in 1x DPBS at 4°C or 1x DPBS containing 50% glycerol at -20°C prior to use.

Control APC755 tetramers were created by first conjugating streptavidin-APC conjugated with NHS-DyLight 755 (APC755) following the manufacturer's instructions (ThermoFisher Scientific). On average, Streptavidin-APC755 contained 4 - 8 DyLight755 molecules per APC. Streptavidin-APC755 was subsequently mixed with biotinylated control antigen and stored at 0.1-1 µM in 1x DPBS at 4°C or in 1x DPBS containing 50% glycerol at -20°C prior to use.

Murine RBD Tetramer-binding B cell enrichment and flow cytometry

The spleen and inguinal, axillary, brachial, cervical, mesenteric, and periaortic lymph nodes from two-four mice were pooled, shredded using forceps, and forced through 100-micron mesh twice to generate filtered single cell suspensions. Cell suspensions were then centrifugated at 300 × g for five minutes at 4°C and supernatant discarded. Pellets were resuspended in 1.2 mL ice cold FACS buffer (1x DPBS containing 1% heat-inactivated newborn calf serum) and divided into twelve 0.1 mL fractions. Each fraction received 2 µg of anti-Fc receptor antibody 2.4G2 (Bio X Cell) and 0.75 pmol of control APC755 tetramer before incubation on ice for 5 minutes. Next, 0.25 pmol RBD APC tetramer, 0.2 µg anti-CD3 BV510 (145-2C11, BD Biosciences), 0.2 µg anti-F4/80 BV510 (BM8, BioLegend), and 0.2 µg anti-Gr-1 BV510 (RB6-8C5, BD Biosciences), 0.3 µg anti-CD19 BUV737 (1D3, BD Biosciences), 0.4 µg anti-B220 BV786 or Pacific Blue (RA3-6B2, BioLegend), and 0.5 µL Fixable Viability Stain 620 (BD Biosciences) were added and samples incubated for 25 minutes on ice. After the incubation, ~15 mL of FACS buffer was added and the samples centrifuged at 300 × g for five minutes at 4°C. The supernatant was discarded, and the pellet resuspended prior to the addition of 8.33 µL of anti-APC microbeads (Miltenyi Biotec). Following a 30 minute incubation on ice, 5 mL of FACS buffer was added and the samples were passed over a magnetized LS column (Miltenyi Biotec). The tube and column were washed once with 5 mL FACS buffer and then removed from the magnetic field. Five mL of FACS buffer was forced through the column with a plunger twice to elute column-bound cells. Following 4°C centrifugation at 300 × g for five minutes, supernatants were discarded and all of the cells from the column-bound fraction and 1/40th of the column flow through were mixed with 20,000 Fluorescent AccuCheck counting beads (ThermoFisher Scientific) to calculate the number of tetramer binding B cells in the column bound fraction, and the total number of B cells in both the column bound and flow through fraction, with the latter multiplied by 40 to account for the 1/40th of the sample interrogated. Flow cytometry was performed at the Fred Hutch Flow Cytometry Core Service on a 5-laser (355nm, 405nm, 488nm, 561nm, 640nm) LSR II, LSRFortessa or FACSymphony (BD Biosciences).

Human S2P Tetramer-binding B cell enrichment and flow cytometry

PBMCs were isolated via venipuncture and cryopreserved from adult volunteers prior to the COVID-19 pandemic as a part of the Fred Hutchinson Seattle Area Control study or from patients diagnosed with COVID-19 as a part of NCT04338360 and NCT04344977 clinical trials. Institutional Review Board approval was obtained from Fred Hutchinson Cancer Center or the University of Washington, and all participants gave written informed consent. 10^7-10^8 frozen PBMCs were thawed into DMEM containing 10% fetal calf serum, 100 U/ml penicillin and 100 µg/ml streptomycin (all from ThermoFisher Scientific). Suspensions were centrifugated at 300 × g for five minutes at 4°C, supernatant discarded, and the pellet resuspended in 50 µL of FACS buffer per 10^7 cells. Control APC755 tetramers were added at a final concentration of 25 nM in the presence of 2% rat and mouse serum (ThermoFisher Scientific) and incubated at room temperature for 10 minutes. SARS-CoV-2 S2P spike APC tetramers were then added at a final concentration of 5 nM and incubated on ice for 25 minutes, followed by a 10 mL wash with ice-cold FACS buffer. Next, 5 µL of anti-APC-conjugated microbeads were added per 10^7 cells and incubated on ice for 30 minutes, after which, 5 mL of FACS buffer was added and the samples were passed over a magnetized LS column (Miltenyi Biotec). The tube and column were washed once with 5 mL FACS buffer and then removed from the magnetic field. Five mL of FACS buffer was forced through the column with a plunger twice to elute column-bound cells which were centrifugated at 300 × g for five minutes at 4°C and supernatant discarded. Cell pellets were resuspended to 50 µL in FACS buffer containing 6.24 µg/mL anti-IgM FITC (G20–127, BD Biosciences), 2.5 µL anti-CD19 BUV395 (SJ25C1, BD Biosciences), 1 µL anti-CD3 BV711 (UCHT1, BD Biosciences), 1 µL anti-CD14 BV711 (M0P-9, BD Biosciences), 1 µL anti-CD16 BV711 (3G8, BD Biosciences), 2.5 µL anti-CD20 BUV737 (2H7, BD Biosciences), 2.5 µL anti-IgD BV605 (IA6–2, BD Biosciences), 3.125 µg/mL anti-CD27 PE/Cy7 (LG.7F9, eBioscience), and 0.5 µL Ghost Dye Violet 510 (Tonbo Biosciences) and incubated for 25 minutes on ice. After the incubation, ~4 mL of FACS buffer was added and the samples centrifuged at 300 × g for five minutes at 4°C. Supernatants were discarded and cells resuspended in FACS buffer and tetramer-binding B cells were individually sorted using a 5-laser (355nm, 405nm, 488nm, 561nm, 640nm) FACS Aria (BD Biosciences) into empty 96-well low profile PCR plates (Labcon), which were sealed with PCR microplate sealing foil (Eppendorf), and flash frozen prior to storage at -80°C.

B cell receptor sequencing

As described previously (243), frozen PCR plates containing individually sorted B cells were placed on ice prior to the addition of 3 µL per well of reverse transcription (RT) master mix containing 50 µM random hexamers (ThermoFisher Scientific), 0.8 µL of 25 mM deoxyribonucleotide triphosphates (dNTPs; ThermoFisher Scientific), 20 U SuperScript IV RT (ThermoFisher Scientific), 20 U RNaseOUT (ThermoFisher Scientific), 2% Igepal (Sigma-Aldrich), and RNase-free water, after which plates were incubated at 50°C for 1 hour. Following RT, 2 µL of cDNA was added to 19 µL first round PCR reaction mix containing 0.5 U HotStarTaq Polymerase (Qiagen), 0.18 µM of each 3′ reverse primer, 0.27 µM of each 5′ forward primer, 0.29 mM GeneAmp dNTPs (ThermoFisher Scientific), and 1X HotStarTaq reaction buffer (Qiagen) in RNase-free water. After the first round of PCR, 2 µL of the PCR product was added to 19 µL of the second-round PCR reaction mix containing 0.5 U HotStarTaq Polymerase, 0.18 µM of each 3′ reverse primer, 0.27 µM of each 5′ forward primer, 0.29 mM dNTPs and 1X HotStarTaq reaction buffer (Qiagen) in RNase-free water. For heavy and kappa light chains, the PCR program for both first and second round was 50 cycles of 94°C for 30 seconds, 57°C for 30 seconds, and 72°C for 55 seconds, followed by 72°C for 10 minutes. For lambda light chains, the PCR program was 50 cycles of 94°C for 30 seconds, 60°C for 30 seconds, and 72°C for 55 seconds, followed by 72°C for 10 minutes.

From the second round PCR product, 4 µL was run on an agarose gel to confirm the presence of a ~500-base pair heavy chain band or a ~450-base pair light chain band. Five µL from PCR reactions with heavy and light chain amplicons was mixed with 2 µL of ExoSAP-IT (ThermoFisher Scientific) and incubated at 37°C for 15 minutes followed by 80°C for 15 minutes to hydrolyze excess primers and nucleotides. Hydrolyzed second-round PCR products were sequenced by Genewiz with the respective reverse primer used in the second round PCR, and sequences were analyzed using IMGT/V-Quest to identify V, D, and J gene segments. Paired heavy chain VDJ and light chain VJ sequences were cloned into pTT3-derived expression vectors containing the human IgG1, Igκ, or Igλ constant regions using In-Fusion cloning (Clontech) as previously described (244).

Monoclonal antibody production

Secreted IgG was produced by co-transfecting 10^6 293F cells/mL with the paired heavy and light chain expression plasmids at a ratio of 1:1 in Freestyle 293 media using 1 mg/mL PEI Max (Polysciences). Transfected cells were cultured for 7 days with gentle shaking at 37°C. Supernatant was collected by centrifuging cultures at 2,500 × g for 15 minutes followed by filtration through a 0.2 µM filter. Clarified supernatants were incubated with Protein A agarose followed by washing with IgG binding buffer (both from ThermoFisher Scientific). Antibodies were eluted with IgG Elution Buffer (ThermoFisher Scientific) into a neutralization buffer containing 1 M Tris-base pH 9.0. Purified antibody was concentrated and buffer exchanged into 1xDPBS using a 50 kDa Amicon Ultra-15 centrifugal filter.

Bio-Layer Interferometry

Bio-Layer Interferometry (BLI) assays were performed on the Octet.Red instrument (ForteBio) at room temperature with shaking at 500 rpm. For binding analyses, anti-human IgG Fc capture biosensors (ForteBio) were loaded with 10 or 40 µg/mL of purified antibody in kinetics buffer (0.01% bovine serum albumin, 0.02% Tween 20, and 0.005% NaN_3 in 1xDPBS, pH 7.4) for 2.5 minutes. After loading, a baseline was recorded for 1 minute in kinetics buffer. The sensors were then immersed in 62.5 or 500 nM of S2P or RBD in kinetics buffer for 5 minutes to assess association followed by immersion in kinetics buffer for 5 minutes to assess dissociation. A 1:1 binding model using ForteBio data analysis software was used for curve fitting.

Peptide:MHC Tetramers

MHC class I heavy chain (HLA-A2) and β2m recombinant proteins were generated by overexpression in *E. coli* and purification of inclusion bodies following adapted protocol from Gabroczi *et al.* (245). To generate individual peptide:MHC monomer complexes, a refolding reaction was set up in an L-arginine rich, glutathione redox refolding buffer with protease inhibitors in the presence of high concentration of the HLA-A2 restricted UV labile peptide H-KLLT(1051)ILTI-OH (Mimotopes), where 1051 denotes a 3-Amino-3 (2-nitro-phenyl)-propionic acid residue. Briefly, peptide was dissolved in a spinning refolding buffer at 4°C prior to the slow injection of β2m followed by heavy chain protein dissolved in injection buffer (3 M guanidine-HCl, 10 mM Na Acetate and 10 mM EDTA, pH 4.2). The solution was incubated at 4°C with slow stirring for 36 hours with additional heavy chain added in a similar manner at 12 and 24 hours. After incubation, precipitated debris was removed by centrifugation at 4000 × g for 5 minutes followed by filtration through 0.22 µm bottle top filters (Corning). The monomer preparation was then concentrated, and buffer exchanged into 10 mM Tris-HCl (pH 8.0) using 10 kDa MWCO Amicon Ultra-15 centrifugal filters (Millipore Sigma). Biotinylation of monomer was carried out using BirA biotin-protein ligase kit (Avidity) according to manufacturer's protocol. Biotinylated monomer was buffer exchanged and concentrated using 10 kDa MWCO Amicon Ultra-15 centrifugal filters prior to purification using the Superdex 200 HR 10/300 NGC Chromatography System (BioRad). The purified monomer was concentrated and stored at 0.5 mg/mL with 2 mg/mL leupeptin, 1 mg/mL pepstatin, 0.5 M EDTA and 10% sodium azide at -80°C until use. Mouse MHC tetramers were made following the same protocol using mouse MHC H-$2K^b$ heavy chain protein (provided by D. Masopust) and UV labile peptide H-SIINFE(1051)L-OH (Mimotopes).

To generate peptide-specific tetramers, UV exchange reaction was set up as described in Fehlings *et al.* (241). Briefly, 62.5 µM of desired peptide and 500 µg/mL of purified monomer in 50 µL 1x PBS was incubated for 15 minutes at 4°C 4-5 cm from a 365 nm UV lamp (Analytik Jena) followed by overnight incubation at 4°C. Tetramers were created by adding Streptavidin-PE (Invitrogen) or Streptavidin-APC (BioLegend) every 10 minutes while incubating in the dark at room temperature with a final ratio of monomer to Streptavidin-fluorophore conjugate of 4 to 1. Following incubation, 400 µM of d-Biotin (Invitrogen) solution with 10% sodium azide was added to saturate any unbound biotin-binding sites on streptavidin and tetramer was stored at 4°C until use. Total protein concentration of tetramer was determined using Bradford assay kit (BioRad). Peptides used were EBV_{GLC} (GLCTLVAML, Biomatik), $SARS\text{-}CoV2_{YLQ}$ (YLQPRTFLL, Biomatik) and Vaccinia virus B8R (TSYKFESV, Biomatik).

Peptide:MHC tetramer cell staining

Human PBMCs were obtained from patients undergoing routine care following Dartmouth Institutional Review Board approved protocols. Cryopreserved PBMCs were thawed and rested for 2 hours in RPMI containing 10% FBS, 1% L-glutamine, 1% HEPES, 1% non-essential amino acids, 1% sodium pyruvate, 0.01% DNAse and β-mercaptoethanol at 37°C. Cells were then washed with 1x PBS and stained with LIVE/DEAD Blue stain kit (ThermoFisher) for 30 minutes on ice. After splitting the sample into three, cells were centrifuged at 400 × g for 5 minutes at 4°C. The supernatant was discarded, and the cell pellet was stained with different batches of tetramer at 1:100 on ice for 30 minutes. Next, cells were centrifuged to remove supernatant and incubated for 30 minutes on ice in 50 µL FACS buffer (1x PBS with 0.2% BSA and 10% sodium azide) containing anti-CD4 PE-Cy5 (RPA-T4, BioLegend), anti-CD8 APC/Fire750 (SK1, BioLegend), and anti-CD3 AF700 (UCHT1, BioLegend). After incubation, cells were washed twice with 3 mL FACS buffer and fixed in 2% PFA before flow cytometry.

Antibody:bead conjugation and use

For each antibody/bead conjugate, 50 µL of UltraComp eBeads Plus compensation beads (ThermoFisher Scientific) was added to 0.125 µg of control or antigen-specific antibody and incubated for 15 minutes on ice. Two mL of FACS buffer was added and beads centrifuged at 400 × g for five minutes at 4°C. Supernatant was aspirated and beads resuspended in 50 µL of FACS buffer and stored at 4°C. For use, 5 µL of beads were mixed with 45 µL of FACS buffer containing 0.25 pmol of tetramer and incubated for 25 minutes on ice. After the incubation, ~4 mL of FACS buffer was added and the samples centrifuged at 400 × g for five minutes at 4°C. The supernatant was discarded, and the beads resuspended in 0.2 mL FACS buffer for flow cytometry.

For bead cocktails, for each antibody/bead conjugate one drop of UltraComp eBeads compensation beads was added to 0.125 µg of

control or antigen-specific antibodies with 0.125 µg of fluorochrome conjugated antibodies. Four mL of FACS buffer was added and beads centrifuged at 400 × g for five minutes at 4°C. Supernatant was aspirated and in some cases beads were resuspended in 50 µL of FACS buffer prior to the addition of 100 µL of 2% paraformaldehyde and incubation for 18 minutes on ice. Four mL of FACS buffer was added and beads centrifuged at 400 × g for five minutes at 4°C. Supernatant was aspirated and beads resuspended in 50 µL of FACS buffer and stored at 4°C. For use, 3 µL of each bead type were mixed and brought up to 50 µL with FACS buffer containing 0.25 pmol of antigen tetramer or 136 µg/mL of peptide:MHC tetramer and incubated for 25 minutes on ice. After the incubation, ~4 mL of FACS buffer was added and the samples centrifuged at 400 × g for five minutes at 4°C. The supernatant was discarded, and the beads resuspended in 0.2 mL FACS buffer for flow cytometry.

Commercially available control antibodies used in this study were anti-PE (PE001, BioLegend), anti-APC (APC003, BioLegend or eBioAPC-6A2, ThermoFisher Scientific), anti-streptavidin (S10D4, ThermoFisher Scientific or Santa Cruz Biotechnology), anti-FITC (FIT-22, BioLegend), and anti-6xHIS tag DyLight680 (HIS.H8, ThermoFisher Scientific). A08 was identified via single cell antibody sequencing of human PBMC B cells and did not bind RBD when expressed as a secreted IgG1. CV30 is an RBD-specific antibody characterized previously (235), and generously provided by L. Stamatatos. 204, 208, 211 and 215 are anti-RBD-specific antibodies characterized previously (182), and generously provided by M. Pepper and J. Netland. E11, 2B8, 2B11, E1, and E7 were identified via single cell antibody sequencing of human PBMC B cells binding SARS-CoV-2 S2P spike tetramers and confirmed to bind RBD when expressed as a secreted IgG1. 2B5 was identified in the same screen and did not bind RBD when expressed as a secreted IgG1. MHC-specific antibodies used in this study were anti-human β2m (A17082A, BioLegend), anti-human HLA-A2 (BB7.2, BioLegend), anti-human HLA-ABC (W6/32, BioLegend), and anti-mouse H-2K^b (Y3, BioXCell).

Fluorochrome-labeled antibodies used for bead multiplexing included anti-human CD19 BUV395 (SJ25C1, BD Biosciences), anti-human CD19 BUV496 (SJ25C1, BD Biosciences), anti-human CD19 BUV563 (SJ25C1, BD Biosciences), anti-human CD79b BUV661 (HM79b, BD Biosciences), anti-human CD20 BUV737 (2H7, BD Biosciences), anti-human CD20 BUV805 (2H7, BD Biosciences), anti-human CD19 BV421 (HIB19, BD Biosciences), anti-human CD45 BV510 (HI30, BD Biosciences), anti-mouse CD43 BV605 (S7, BD Biosciences), anti-mouse CD93 BV650 (AA4.1, BD Biosciences), anti-human CD3 BV711 (UCHT1, BD Biosciences), anti-human CD19 BV786 (2H7, BD Biosciences), anti-human CD19 FITC (HIB19, BioLegend), anti-mouse B220/CD45R PerCP (RA3-6B2, BD Biosciences), anti-human CD10 PerCP-Cy5.5 (HI10a, BD Biosciences), anti-mouse CD4 BV711 (RM4-5, BioLegend), anti-mouse CD4 BV421 (GK1.5, BioLegend), anti-mouse CD103 APC & BV510 (2E7, BioLegend), anti-mouse Thy1.2 PerCP (53-2.1, BioLegend), anti-mouse CD197 PE (4B12, BioLegend), anti-mouse CD8a BV605 (53-6.7, BioLegend), and anti-mouse PD-1 PE-Cy7 (29F.1, BioLegend).

Figure Generation
Figures were generated using BioRender, FlowJo 10 (Becton Dickinson & Company), Prism 9 (Dotmatics) and Illustrator 2021 (Adobe).

AUTHOR CONTRIBUTIONS

K. S. Fitzpatrick produced antigen tetramers, designed, conducted, and analyzed murine cell and bead experiments; H. N. Degefu produced peptide:MHC tetramers, designed, conducted and analyzed peptide:MHC tetramer cell and bead experiments, generated figures and helped write portions of the manuscript; K. Poljakov conducted murine cell and bead experiments; M. G. Bibby conducted and analyzed BLI experiments; A. J. Remington produced tetramers, designed and conducted bead experiments; T.G. Searles produced peptide:MHC tetramers; M. D. Gray produced, purified, and validated antigens and antibodies; J. Boonyaratanakornkit conducted human cell sorting experiments to clone SARS-CoV-2-specific antibodies, conducted and analyzed BLI experiments, and edited the manuscript; P.C. Rosato designed peptide:MHC tetramer experiments, and wrote and edited portions of the manuscript; J.J. Taylor designed and analyzed experiments, generated figures, and wrote the manuscript.

ACKNOWLEDGMENTS

We thank L. Stamatatos for CV30; M. Pepper and J. Netland for 204, 208, 211 and 215; M. J. McElrath for PBMCs from Seattle Area Control cohort; D. Koelle and A. Wald for COVID-19 PBMC samples from NCT04338360 and NCT04344977; B. Graham for SARS-CoV-2 S2P plasmid; Fred Hutch Flow Cytometry and Comparative Medicine Shared Resource staff for technical assistance; M. Lopez-Bernal, L. Yates, R. Putnam, and M. Gurtovnik for administrative assistance; S. Voght for manuscript editing; and D. Baumjohann, A. Broggi, K. Bruton, C. Castellanos, L. Chopp, C. Coelho, D. Glass, C. Hopp, J. Koenig, S. Langel, N. Mohamed, K. O'Connor, G. Rizzuto, C. Sundling, L. Swadling, P. Wilson, F. Wimmers, R. Yefet, and T. Yewdell for suggesting important citations on Twitter or through email; the bioMT Molecular Tools Core at Dartmouth for help with peptide:MHC monomer production; E. Ferris and M. Cole for use of their FPLC; the NIH tetramer core for *E.coli* expressing HLA-A2 heavy chain; D. Masopust for *E.coli* expressing mouse H2K^b and human β2m; and E. Newell for helpful discussions regarding MHC tetramer production. Research reported in this publication was supported by the National Institutes of Health under award numbers R01AI122912 to J.J. Taylor, T32GM095421 to K. Fitzpatrick, P20GM13132-07 to P.C. Rosato, Fast Grants award to J. Boonyaratanakornkit, and a Fred Hutch Evergreen award to J. Boonyaratanakornkit & J. J. Taylor.

REFERENCES

1. Julius, M.H., Masuda, T., and Herzenberg, L.A. (1972). Demonstration that antigen-binding cells are precursors of antibody-producing cells after purification with a fluorescence-activated cell sorter. Proc Natl Acad Sci U S A *69*, 1934-1938. 10.1073/pnas.69.7.1934.

2. Greenstein, J.L., Leary, J., Horan, P., Kappler, J.W., and Marrack, P. (1980). Flow sorting of antigen-binding B cell subsets. J Immunol *124*, 1472-1481.

3. Hayakawa, K., Ishii, R., Yamasaki, K., Kishimoto, T., and Hardy, R.R. (1987). Isolation of high-affinity memory B cells: phycoerythrin as a probe for antigen-binding cells. Proc Natl Acad Sci U S A *84*, 1379-1383. 10.1073/pnas.84.5.1379.

4. Goodnow, C.C., Crosbie, J., Adelstein, S., Lavoie, T.B., Smith-Gill, S.J., Brink, R.A., Pritchard-Briscoe, H., Wotherspoon, J.S., Loblay, R.H., Raphael, K., Trent, R.J., and Basten, A. (1988). Altered immunoglobulin expression and functional silencing of self-reactive B lymphocytes in transgenic mice. Nature *334*, 676-682. 10.1038/334676a0.

5. Hoven, M.Y., De Leij, L., Keij, J.F., and The, T.H. (1989). Detection and isolation of antigen-specific B cells by the fluorescence activated cell sorter (FACS). J Immunol Methods *117*, 275-284. 10.1016/0022-1759(89)90150-6.

6. Schittek, B., and Rajewsky, K. (1990). Maintenance of B-cell memory by long-lived cells generated from proliferating precursors. Nature *346*, 749-751. 10.1038/346749a0.

7. Erikson, J., Radic, M.Z., Camper, S.A., Hardy, R.R., Carmack, C., and Weigert, M. (1991). Expression of anti-DNA immunoglobulin transgenes in non-autoimmune mice. Nature *349*, 331-334. 10.1038/349331a0.

8. McHeyzer-Williams, M.G., Nossal, G.J., and Lalor, P.A. (1991). Molecular characterization of single memory B cells. Nature *350*, 502-505. 10.1038/350502a0.

9. Brink, R., Goodnow, C.C., Crosbie, J., Adams, E., Eris, J., Mason, D.Y., Hartley, S.B., and Basten, A. (1992). Immunoglobulin M and D antigen receptors are both capable of mediating B lymphocyte activation, deletion, or anergy after interaction with specific antigen. J Exp Med *176*, 991-1005. 10.1084/jem.176.4.991.

10. Lalor, P.A., Nossal, G.J., Sanderson, R.D., and McHeyzer-Williams, M.G. (1992). Functional and molecular characterization of single, (4-hydroxy-3-nitrophenyl)acetyl (NP)-specific, IgG1+ B cells from antibody-secreting and memory B cell pathways in the C57BL/6 immune response to NP. Eur J Immunol *22*, 3001-3011. 10.1002/eji.1830221136.

11. Fulcher, D.A., and Basten, A. (1994). Reduced life span of anergic self-reactive B cells in a double-transgenic model. J Exp Med *179*, 125-134.

12. Rathmell, J.C., Cooke, M.P., Ho, W.Y., Grein, J., Townsend, S.E., Davis, M.M., and Goodnow, C.C. (1995). CD95 (Fas)-dependent elimination of self-reactive B cells upon interaction with CD4+ T cells. Nature *376*, 181-184. 10.1038/376181a0.

13. Cook, M.C., Basten, A., and Fazekas de St Groth, B. (1998). Rescue of self-reactive B cells by provision of T cell help in vivo. Eur J Immunol *28*, 2549-2558. 10.1002/(SICI)1521-4141(199808)28:08<2549::AID-IMMU2549>3.0.CO;2-O.

14. Litzenburger, T., Fassler, R., Bauer, J., Lassmann, H., Linington, C., Wekerle, H., and Iglesias, A. (1998). B lymphocytes producing demyelinating autoantibodies: development and function in gene-targeted transgenic mice. J Exp Med *188*, 169-180. 10.1084/jem.188.1.169.

15. Ridderstad, A., and Tarlinton, D.M. (1998). Kinetics of establishing the memory B cell population as revealed by CD38 expression. J Immunol *160*, 4688-4695.

16. Hannum, L.G., Haberman, A.M., Anderson, S.M., and Shlomchik, M.J. (2000). Germinal center initiation, variable gene region hypermutation, and mutant B cell selection without detectable immune complexes on follicular dendritic cells. J Exp Med *192*, 931-942. 10.1084/jem.192.7.931.

17. Maruyama, M., Lam, K.P., and Rajewsky, K. (2000). Memory B-cell persistence is independent of persisting immunizing antigen. Nature *407*, 636-642. 10.1038/35036600.

18. McHeyzer-Williams, M.G., McHeyzer-Williams, L.J., Fanelli Panus, J., Bikah, G., Pogue-Caley, R.R., Driver, D.J., and Eisenbraun, M.D. (2000). Antigen-specific immunity. Th cell-dependent B cell responses. Immunol Res *22*, 223-236. 10.1385/IR:22:2-3:223.

19. Benschop, R.J., Aviszus, K., Zhang, X., Manser, T., Cambier, J.C., and Wysocki, L.J. (2001). Activation and anergy in bone marrow B cells of a novel immunoglobulin transgenic mouse that is both hapten specific and autoreactive. Immunity *14*, 33-43. 10.1016/s1074-7613(01)00087-5.

20. Martin, F., Oliver, A.M., and Kearney, J.F. (2001). Marginal zone and B1 B cells unite in the early response against T-independent blood-borne particulate antigens. Immunity *14*, 617-629. 10.1016/s1074-7613(01)00129-7.

21. Townsend, S.E., Goodnow, C.C., and Cornall, R.J. (2001). Single epitope multiple staining to detect ultralow frequency B cells. J Immunol Methods *249*, 137-146. 10.1016/s0022-1759(00)00352-5.

22. Bell, J., and Gray, D. (2003). Antigen-capturing cells can masquerade as memory B cells. J Exp Med *197*, 1233-1244. 10.1084/jem.20020270.

23. Newman, J., Rice, J.S., Wang, C., Harris, S.L., and Diamond, B. (2003). Identification of an antigen-specific B cell population. J Immunol Methods *272*, 177-187. 10.1016/s0022-1759(02)00499-4.

24. Phan, T.G., Amesbury, M., Gardam, S., Crosbie, J., Hasbold, J., Hodgkin, P.D., Basten, A., and Brink, R. (2003). B cell receptor-independent stimuli trigger immunoglobulin (Ig) class switch recombination and production of IgG autoantibodies by anergic self-reactive B cells. J Exp Med *197*, 845-860. 10.1084/jem.20022144.

25. Weitkamp, J.H., Kallewaard, N., Kusuhara, K., Feigelstock, D., Feng, N., Greenberg, H.B., and Crowe, J.E., Jr. (2003). Generation of recombinant human monoclonal antibodies to rotavirus from single antigen-specific B cells selected with fluorescent virus-like particles. J Immunol Methods *275*, 223-237. 10.1016/s0022-1759(03)00013-9.

26. Lesley, R., Xu, Y., Kalled, S.L., Hess, D.M., Schwab, S.R., Shu, H.B., and Cyster, J.G. (2004). Reduced competitiveness of autoantigen-engaged B cells due to increased dependence on BAFF. Immunity *20*, 441-453. 10.1016/s1074-7613(04)00079-2.

27. Acevedo-Suarez, C.A., Hulbert, C., Woodward, E.J., and Thomas, J.W. (2005). Uncoupling of anergy from developmental arrest in anti-insulin B cells supports the development of autoimmune diabetes. J Immunol *174*, 827-833. 10.4049/jimmunol.174.2.827.

28. Odendahl, M., Mei, H., Hoyer, B.F., Jacobi, A.M., Hansen, A., Muehlinghaus, G., Berek, C., Hiepe, F., Manz, R., Radbruch, A., and Dorner, T. (2005). Generation of migratory antigen-specific plasma blasts and mobilization of resident plasma cells in a secondary immune response. Blood *105*, 1614-1621. 10.1182/blood-2004-07-2507.

29. Hsu, M.C., Toellner, K.M., Vinuesa, C.G., and Maclennan, I.C. (2006). B cell clones that sustain long-term plasmablast growth in T-independent extrafollicular antibody responses. Proc Natl Acad Sci U S A *103*, 5905-5910. 10.1073/pnas.0601502103.

30. O'Connor, B.P., Vogel, L.A., Zhang, W., Loo, W., Shnider, D., Lind, E.F., Ratliff, M., Noelle, R.J., and Erickson, L.D. (2006). Imprinting the fate of antigen-reactive B cells through the affinity of the B cell receptor. J Immunol *177*, 7723-7732. 10.4049/jimmunol.177.11.7723.

31. Anderson, S.M., Tomayko, M.M., Ahuja, A., Haberman, A.M., and Shlomchik, M.J. (2007). New markers for murine memory B cells that define mutated and unmutated subsets. J Exp Med *204*, 2103-2114. 10.1084/jem.20062571.

32. Pape, K.A., Catron, D.M., Itano, A.A., and Jenkins, M.K. (2007). The humoral immune response is initiated in lymph nodes by B cells that acquire soluble antigen directly in the follicles. Immunity *26*, 491-502. 10.1016/j.immuni.2007.02.011.

33. Benson, M.J., Elgueta, R., Schpero, W., Molloy, M., Zhang, W., Usherwood, E., and Noelle, R.J. (2009). Distinction of the memory B cell response to cognate antigen versus bystander inflammatory signals. J Exp Med *206*, 2013-2025. 10.1084/jem.20090667.

34. Dogan, I., Bertocci, B., Vilmont, V., Delbos, F., Megret, J., Storck, S., Reynaud, C.A., and Weill, J.C. (2009). Multiple layers of B cell memory with different effector functions. Nat Immunol *10*, 1292-1299. 10.1038/ni.1814.

35. Scheid, J.F., Mouquet, H., Feldhahn, N., Seaman, M.S., Velinzon, K., Pietzsch, J., Ott, R.G., Anthony, R.M., Zebroski, H., Hurley, A., Phogat, A., Chakrabarti, B., Li, Y., Connors, M., Pereyra, F., Walker, B.D., Wardemann, H., Ho, D., Wyatt, R.T., Mascola, J.R., Ravetch, J.V., and Nussenzweig, M.C. (2009). Broad diversity of neutralizing antibodies isolated from memory B cells in HIV-infected individuals. Nature *458*, 636-640. 10.1038/nature07930.

36. Frolich, D., Giesecke, C., Mei, H.E., Reiter, K., Daridon, C., Lipsky, P.E., and Dorner, T. (2010). Secondary immunization generates clonally related antigen-specific plasma cells and memory B cells. J Immunol *185*, 3103-3110. 10.4049/jimmunol.1000911.

37. Good-Jacobson, K.L., Szumilas, C.G., Chen, L., Sharpe, A.H., Tomayko, M.M., and Shlomchik, M.J. (2010). PD-1 regulates germinal center B cell survival and the formation and affinity of long-lived plasma cells. Nat Immunol *11*, 535-542. 10.1038/ni.1877.

38. Kwakkenbos, M.J., Diehl, S.A., Yasuda, E., Bakker, A.Q., van Geelen, C.M., Lukens, M.V., van Bleek, G.M., Widjojoatmodjo, M.N., Bogers, W.M., Mei, H., Radbruch, A., Scheeren, F.A., Spits, H., and Beaumont, T. (2010). Generation of stable monoclonal antibody-producing B cell receptor-positive human memory B cells by genetic programming. Nat Med *16*, 123-128. 10.1038/nm.2071.

39. Franz, B., May, K.F., Jr., Dranoff, G., and Wucherpfennig, K. (2011). Ex vivo characterization and isolation of rare memory B cells with antigen tetramers. Blood *118*, 348-357. 10.1182/blood-2011-03-341917.

40. Hou, B., Saudan, P., Ott, G., Wheeler, M.L., Ji, M., Kuzmich, L., Lee, L.M., Coffman, R.L., Bachmann, M.F., and DeFranco, A.L. (2011). Selective utilization of Toll-like receptor and MyD88 signaling in B cells for enhancement of the antiviral germinal center response. Immunity *34*, 375-384. 10.1016/j.immuni.2011.01.011.

41. Lee, S.K., Rigby, R.J., Zotos, D., Tsai, L.M., Kawamoto, S., Marshall, J.L., Ramiscal, R.R., Chan, T.D., Gatto, D., Brink, R., Yu, D., Fagarasan, S., Tarlinton, D.M., Cunningham, A.F., and Vinuesa, C.G. (2011). B cell priming for extrafollicular antibody responses requires Bcl-6 expression by T cells. J Exp Med *208*, 1377-1388. 10.1084/jem.20102065.

42. Pape, K.A., Taylor, J.J., Maul, R.W., Gearhart, P.J., and Jenkins, M.K. (2011). Different B cell populations mediate early and late memory during an endogenous immune response. Science *331*, 1203-1207. 10.1126/science.1201730.

43. Dougan, S.K., Ogata, S., Hu, C.C., Grotenbreg, G.M., Guillen, E., Jaenisch, R., and Ploegh, H.L. (2012). IgG1+ ovalbumin-specific B-cell transnuclear mice show class switch recombination in rare allelically included B cells. Proc Natl Acad Sci U S A *109*, 13739-13744. 10.1073/pnas.1210273109.

44. Khaskhely, N., Mosakowski, J., Thompson, R.S., Khuder, S., Smithson, S.L., and Westerink, M.A. (2012). Phenotypic analysis of pneumococcal polysaccharide-specific B cells. J Immunol *188*, 2455-2463. 10.4049/jimmunol.1102809.

45. Moody, M.A., Yates, N.L., Amos, J.D., Drinker, M.S., Eudailey, J.A., Gurley, T.C., Marshall, D.J., Whitesides, J.F., Chen, X., Foulger, A., Yu, J.S., Zhang, R., Meyerhoff, R.R., Parks, R., Scull, J.C., Wang, L., Vandergrift, N.A., Pickeral, J., Pollara, J., Kelsoe, G., Alam, S.M., Ferrari, G., Montefiori, D.C., Voss, G., Liao, H.X., Tomaras, G.D., and Haynes, B.F. (2012). HIV-1 gp120 vaccine induces affinity maturation in both new and persistent antibody clonal lineages. J Virol *86*, 7496-7507. 10.1128/JVI.00426-12.

46. Sholukh, A.M., Mukhtar, M.M., Humbert, M., Essono, S.S., Watkins, J.D., Vyas, H.K., Shanmuganathan, V., Hemashettar, G., Kahn, M., Hu, S.L., Montefiori, D.C., Polonis, V.R., Schur, P.H., and Ruprecht, R.M. (2012). Isolation of monoclonal antibodies with predetermined conformational epitope specificity. PLoS One *7*, e38943. 10.1371/journal.pone.0038943.

47. Sundling, C., Li, Y., Huynh, N., Poulsen, C., Wilson, R., O'Dell, S., Feng, Y., Mascola, J.R., Wyatt, R.T., and Karlsson Hedestam, G.B. (2012). High-resolution definition of vaccine-elicited B cell responses against the HIV primary receptor binding site. Sci Transl Med *4*, 142ra196. 10.1126/scitranslmed.3003752.

48. Taylor, J.J., Martinez, R.J., Titcombe, P.J., Barsness, L.O., Thomas, S.R., Zhang, N., Katzman, S.D., Jenkins, M.K., and Mueller, D.L. (2012). Deletion and anergy of polyclonal B cells specific for ubiquitous membrane-bound self-antigen. J Exp Med *209*, 2065-2077. 10.1084/jem.20112272.

49. Taylor, J.J., Pape, K.A., and Jenkins, M.K. (2012). A germinal center-independent pathway generates unswitched memory B cells early in the primary response. J Exp Med *209*, 597-606. 10.1084/jem.20111696.

50. Dougan, S.K., Ashour, J., Karssemeijer, R.A., Popp, M.W., Avalos, A.M., Barisa, M., Altenburg, A.F., Ingram, J.R., Cragnolini, J.J., Guo, C., Alt, F.W., Jaenisch, R., and Ploegh, H.L. (2013). Antigen-specific B-cell receptor sensitizes B cells to infection by influenza virus. Nature *503*, 406-409. 10.1038/nature12637.

51. Doyle-Cooper, C., Hudson, K.E., Cooper, A.B., Ota, T., Skog, P., Dawson, P.E., Zwick, M.B., Schief, W.R., Burton, D.R., and Nemazee, D. (2013). Immune tolerance negatively regulates B cells in knock-in mice expressing broadly neutralizing HIV antibody 4E10. J Immunol *191*, 3186-3191. 10.4049/jimmunol.1301285.

52. Haasken, S., Auger, J.L., Taylor, J.J., Hobday, P.M., Goudy, B.D., Titcombe, P.J., Mueller, D.L., and Binstadt, B.A. (2013). Macrophage scavenger receptor 1 (Msr1, SR-A) influences B cell autoimmunity by regulating soluble autoantigen concentration. J Immunol *191*, 1055-1062. 10.4049/jimmunol.1201680.

53. Klein, F., Diskin, R., Scheid, J.F., Gaebler, C., Mouquet, H., Georgiev, I.S., Pancera, M., Zhou, T., Incesu, R.B., Fu, B.Z., Gnanapragasam, P.N., Oliveira, T.Y., Seaman, M.S., Kwong, P.D., Bjorkman, P.J., and Nussenzweig, M.C. (2013). Somatic mutations of the immunoglobulin framework are generally required for broad and potent HIV-1 neutralization. Cell *153*, 126-138. 10.1016/j.cell.2013.03.018.

54. Ota, T., Doyle-Cooper, C., Cooper, A.B., Doores, K.J., Aoki-Ota, M., Le, K., Schief, W.R., Wyatt, R.T., Burton, D.R., and Nemazee, D. (2013). B cells from knock-in mice expressing broadly neutralizing HIV antibody b12 carry an innocuous B cell receptor responsive to HIV vaccine candidates. J Immunol *191*, 3179-3185. 10.4049/jimmunol.1301283.

55. Sahaf, B., Yang, Y., Arai, S., Herzenberg, L.A., Herzenberg, L.A., and Miklos, D.B. (2013). H-Y antigen-binding B cells develop in male recipients of female hematopoietic cells and associate with chronic graft vs. host disease. Proc Natl Acad Sci U S A *110*, 3005-3010. 10.1073/pnas.1222900110.

56. Verkoczy, L., Chen, Y., Zhang, J., Bouton-Verville, H., Newman, A., Lockwood, B., Scearce, R.M., Montefiori, D.C., Dennison, S.M., Xia, S.M., Hwang, K.K., Liao, H.X., Alam, S.M., and Haynes, B.F. (2013). Induction of HIV-1 broad neutralizing antibodies in 2F5 knock-in mice: selection against membrane proximal external region-associated autoreactivity limits T-dependent responses. J Immunol *191*, 2538-2550. 10.4049/jimmunol.1300971.

57. Chung, J.Y., Figgett, W., Fairfax, K., Bernard, C., Chan, J., Toh, B.H., Mackay, F., and Alderuccio, F. (2014). Gene therapy delivery of myelin oligodendrocyte glycoprotein (MOG) via hematopoietic stem cell transfer induces MOG-specific B cell deletion. J Immunol *192*, 2593-2601. 10.4049/jimmunol.1203563.

58. Conter, L.J., Song, E., Shlomchik, M.J., and Tomayko, M.M. (2014). CD73 expression is dynamically regulated in the germinal center and bone marrow plasma cells are diminished in its absence. PLoS One *9*, e92009. 10.1371/journal.pone.0092009.

59. Giesecke, C., Frolich, D., Reiter, K., Mei, H.E., Wirries, I., Kuhly, R., Killig, M., Glatzer, T., Stolzel, K., Perka, C., Lipsky, P.E., and Dorner, T. (2014). Tissue distribution and dependence of responsiveness of human antigen-specific memory B cells. J Immunol *192*, 3091-3100. 10.4049/jimmunol.1302783.

60. Good-Jacobson, K.L., Chen, Y., Voss, A.K., Smyth, G.K., Thomas, T., and Tarlinton, D. (2014). Regulation of germinal center responses and B-cell memory by the chromatin modifier MOZ. Proc Natl Acad Sci U S A *111*, 9585-9590. 10.1073/pnas.1402485111.

61. Sabouri, Z., Schofield, P., Horikawa, K., Spierings, E., Kipling, D., Randall, K.L., Langley, D., Roome, B., Vazquez-Lombardi, R., Rouet, R., Hermes, J., Chan, T.D., Brink, R., Dunn-Walters, D.K., Christ, D., and Goodnow, C.C. (2014). Redemption of autoantibodies on anergic B cells by variable-region glycosylation and mutation away from self-reactivity. Proc Natl Acad Sci U S A *111*, E2567-2575. 10.1073/pnas.1406974111.

62. Scherer, E.M., Smith, R.A., Simonich, C.A., Niyonzima, N., Carter, J.J., and Galloway, D.A. (2014). Characteristics of memory B cells elicited by a highly efficacious HPV vaccine in subjects with no pre-existing immunity. PLoS Pathog *10*, e1004461. 10.1371/journal.ppat.1004461.

63. Sundling, C., Zhang, Z., Phad, G.E., Sheng, Z., Wang, Y., Mascola, J.R., Li, Y., Wyatt, R.T., Shapiro, L., and Karlsson Hedestam, G.B. (2014). Single-cell and deep sequencing of IgG-switched macaque B cells reveal a diverse Ig repertoire following immunization. J Immunol *192*, 3637-3644. 10.4049/jimmunol.1303334.

64. Taylor, J.J., Laudenbach, M., Tucker, A.M., Jenkins, M.K., and Pravetoni, M. (2014). Hapten-specific naive B cells are biomarkers of vaccine efficacy against drugs of abuse. J Immunol Methods *405*, 74-86. 10.1016/j.jim.2014.01.010.

65. Whittle, J.R., Wheatley, A.K., Wu, L., Lingwood, D., Kanekiyo, M., Ma, S.S., Narpala, S.R., Yassine, H.M., Frank, G.M., Yewdell, J.W., Ledgerwood, J.E., Wei, C.J., McDermott, A.B., Graham, B.S., Koup, R.A., and Nabel, G.J. (2014). Flow cytometry reveals that H5N1 vaccination elicits cross-reactive stem-directed antibodies from multiple Ig heavy-chain lineages. J Virol *88*, 4047-4057. 10.1128/JVI.03422-13.

66. Zuccarino-Catania, G.V., Sadanand, S., Weisel, F.J., Tomayko, M.M., Meng, H., Kleinstein, S.H., Good-Jacobson, K.L., and Shlomchik, M.J. (2014). CD80 and PD-L2 define functionally distinct memory B cell subsets that are independent of antibody isotype. Nat Immunol *15*, 631-637. 10.1038/ni.2914.

67. Brink, R., Paus, D., Bourne, K., Hermes, J.R., Gardam, S., Phan, T.G., and Chan, T.D. (2015). The SW(HEL) system for high-resolution analysis of in vivo antigen-specific T-dependent B cell responses. Methods Mol Biol *1291*, 103-123. 10.1007/978-1-4939-2498-1_9.

68. Hamilton, J.A., Li, J., Wu, Q., Yang, P., Luo, B., Li, H., Bradley, J.E., Taylor, J.J., Randall, T.D., Mountz, J.D., and Hsu, H.C. (2015). General Approach for Tetramer-Based Identification of Autoantigen-Reactive B Cells: Characterization of La- and snRNP-Reactive B Cells in Autoimmune BXD2 Mice. J Immunol *194*, 5022-5034. 10.4049/jimmunol.1402335.

69. Jones, D.D., Wilmore, J.R., and Allman, D. (2015). Cellular Dynamics of Memory B Cell Populations: IgM+ and IgG+ Memory B Cells Persist Indefinitely as Quiescent Cells. J Immunol *195*, 4753-4759. 10.4049/jimmunol.1501365.

70. Laudenbach, M., Baruffaldi, F., Vervacke, J.S., Distefano, M.D., Titcombe, P.J., Mueller, D.L., Tubo, N.J., Griffith, T.S., and Pravetoni, M. (2015). The frequency of naive and early-activated hapten-specific B cell subsets dictates the efficacy of a therapeutic vaccine against prescription opioid abuse. J Immunol *194*, 5926-5936. 10.4049/jimmunol.1500385.

71. McHeyzer-Williams, L.J., Milpied, P.J., Okitsu, S.L., and McHeyzer-Williams, M.G. (2015). Class-switched memory B cells remodel BCRs within secondary germinal centers. Nat Immunol *16*, 296-305. 10.1038/ni.3095.

72. Nanton, M.R., Lee, S.J., Atif, S.M., Nuccio, S.P., Taylor, J.J., Baumler, A.J., Way, S.S., and McSorley, S.J. (2015). Direct visualization of endogenous Salmonella-specific B cells reveals a marked delay in clonal expansion and germinal center development. Eur J Immunol *45*, 428-441. 10.1002/eji.201444540.

73. Patil, S.U., Ogunniyi, A.O., Calatroni, A., Tadigotla, V.R., Ruiter, B., Ma, A., Moon, J., Love, J.C., and Shreffler, W.G. (2015). Peanut oral immunotherapy transiently expands circulating Ara h 2-specific B cells with a homologous repertoire in unrelated subjects. J Allergy Clin Immunol *136*, 125-134 e112. 10.1016/j.jaci.2015.03.026.

74. Smith, M.J., Packard, T.A., O'Neill, S.K., Henry Dunand, C.J., Huang, M., Fitzgerald-Miller, L., Stowell, D., Hinman, R.M., Wilson, P.C., Gottlieb, P.A., and Cambier, J.C. (2015). Loss of anergic B cells in prediabetic and new-onset type 1 diabetic patients. Diabetes *64*, 1703-1712. 10.2337/db13-1798.

75. Taylor, J.J., Pape, K.A., Steach, H.R., and Jenkins, M.K. (2015). Humoral immunity. Apoptosis and antigen affinity limit effector cell differentiation of a single naive B cell. Science *347*, 784-787. 10.1126/science.aaa1342.

76. Bornholdt, Z.A., Turner, H.L., Murin, C.D., Li, W., Sok, D., Souders, C.A., Piper, A.E., Goff, A., Shamblin, J.D., Wollen, S.E., Sprague, T.R., Fusco, M.L., Pommert, K.B., Cavacini, L.A., Smith, H.L., Klempner, M., Reimann, K.A., Krauland, E., Gerngross, T.U., Wittrup, K.D., Saphire, E.O., Burton, D.R., Glass, P.J., Ward, A.B., and Walker, L.M. (2016). Isolation of potent neutralizing antibodies from a survivor of the 2014 Ebola virus outbreak. Science *351*, 1078-1083. 10.1126/science.aad5788.

77. Chou, C., Verbaro, D.J., Tonc, E., Holmgren, M., Cella, M., Colonna, M., Bhattacharya, D., and Egawa, T. (2016). The Transcription Factor AP4 Mediates Resolution of Chronic Viral Infection through Amplification of Germinal Center B Cell Responses. Immunity *45*, 570-582. 10.1016/j.immuni.2016.07.023.

78. Ellebedy, A.H., Jackson, K.J., Kissick, H.T., Nakaya, H.I., Davis, C.W., Roskin, K.M., McElroy, A.K., Oshansky, C.M., Elbein, R., Thomas, S., Lyon, G.M., Spiropoulou, C.F., Mehta, A.K., Thomas, P.G., Boyd, S.D., and Ahmed, R. (2016). Defining antigen-specific plasmablast and memory B cell subsets in human blood after viral infection or vaccination. Nat Immunol *17*, 1226-1234. 10.1038/ni.3533.

79. Gilman, M.S., Castellanos, C.A., Chen, M., Ngwuta, J.O., Goodwin, E., Moin, S.M., Mas, V., Melero, J.A., Wright, P.F., Graham, B.S., McLellan, J.S., and Walker, L.M. (2016). Rapid profiling of RSV antibody repertoires from the memory B cells of naturally infected adult donors. Sci Immunol *1*. 10.1126/sciimmunol.aaj1879.

80. Gitlin, A.D., von Boehmer, L., Gazumyan, A., Shulman, Z., Oliveira, T.Y., and Nussenzweig, M.C. (2016). Independent Roles of Switching and Hypermutation in the Development and Persistence of B Lymphocyte Memory. Immunity *44*, 769-781. 10.1016/j.immuni.2016.01.011.

81. Guy, T.V., Terry, A.M., Bolton, H.A., Hancock, D.G., Zhu, E., Brink, R., McGuire, H.M., Shklovskaya, E., and Fazekas de St. Groth, B. (2016). Collaboration between tumor-specific CD4+ T cells and B cells

in anti-cancer immunity. Oncotarget *7*, 30211-30229. 10.18632/oncotarget.8797.

82. Jash, A., Wang, Y., Weisel, F.J., Scharer, C.D., Boss, J.M., Shlomchik, M.J., and Bhattacharya, D. (2016). ZBTB32 Restricts the Duration of Memory B Cell Recall Responses. J Immunol *197*, 1159-1168. 10.4049/jimmunol.1600882.

83. Joshua, V., Schobers, L., Titcombe, P.J., Israelsson, L., Ronnelid, J., Hansson, M., Catrina, A.I., Pruijn, G.J., and Malmstrom, V. (2016). Antibody responses to de novo identified citrullinated fibrinogen peptides in rheumatoid arthritis and visualization of the corresponding B cells. Arthritis Res Ther *18*, 284. 10.1186/s13075-016-1181-0.

84. Keitany, G.J., Kim, K.S., Krishnamurty, A.T., Hondowicz, B.D., Hahn, W.O., Dambrauskas, N., Sather, D.N., Vaughan, A.M., Kappe, S.H.I., and Pepper, M. (2016). Blood Stage Malaria Disrupts Humoral Immunity to the Pre-erythrocytic Stage Circumsporozoite Protein. Cell Rep *17*, 3193-3205. 10.1016/j.celrep.2016.11.060.

85. Krishnamurty, A.T., Thouvenel, C.D., Portugal, S., Keitany, G.J., Kim, K.S., Holder, A., Crompton, P.D., Rawlings, D.J., and Pepper, M. (2016). Somatically Hypermutated Plasmodium-Specific IgM(+) Memory B Cells Are Rapid, Plastic, Early Responders upon Malaria Rechallenge. Immunity *45*, 402-414. 10.1016/j.immuni.2016.06.014.

86. Malkiel, S., Jeganathan, V., Wolfson, S., Manjarrez Orduno, N., Marasco, E., Aranow, C., Mackay, M., Gregersen, P.K., and Diamond, B. (2016). Checkpoints for Autoreactive B Cells in the Peripheral Blood of Lupus Patients Assessed by Flow Cytometry. Arthritis Rheumatol *68*, 2210-2220. 10.1002/art.39710.

87. Onodera, T., Hosono, A., Odagiri, T., Tashiro, M., Kaminogawa, S., Okuno, Y., Kurosaki, T., Ato, M., Kobayashi, K., and Takahashi, Y. (2016). Whole-Virion Influenza Vaccine Recalls an Early Burst of High-Affinity Memory B Cell Response through TLR Signaling. J Immunol *196*, 4172-4184. 10.4049/jimmunol.1600046.

88. Shinnakasu, R., Inoue, T., Kometani, K., Moriyama, S., Adachi, Y., Nakayama, M., Takahashi, Y., Fukuyama, H., Okada, T., and Kurosaki, T. (2016). Regulated selection of germinal-center cells into the memory B cell compartment. Nat Immunol *17*, 861-869. 10.1038/ni.3460.

89. Spanier, J.A., Frederick, D.R., Taylor, J.J., Heffernan, J.R., Kotov, D.I., Martinov, T., Osum, K.C., Ruggiero, J.L., Rust, B.J., Landry, S.J., Jenkins, M.K., McLachlan, J.B., and Fife, B.T. (2016). Efficient generation of monoclonal antibodies against peptide in the context of MHCII using magnetic enrichment. Nat Commun *7*, 11804. 10.1038/ncomms11804.

90. Weisel, F.J., Zuccarino-Catania, G.V., Chikina, M., and Shlomchik, M.J. (2016). A Temporal Switch in the Germinal Center Determines Differential Output of Memory B and Plasma Cells. Immunity *44*, 116-130. 10.1016/j.immuni.2015.12.004.

91. Angeletti, D., Frank, G.M., and Yewdell, J.W. (2017). Flow-Cytometric Method Measuring B Cell Surface Immunoglobulin Avidity. Methods Mol Biol *1623*, 181-189. 10.1007/978-1-4939-7095-7_15.

92. Angeletti, D., Gibbs, J.S., Angel, M., Kosik, I., Hickman, H.D., Frank, G.M., Das, S.R., Wheatley, A.K., Prabhakaran, M., Leggat, D.J., McDermott, A.B., and Yewdell, J.W. (2017). Defining B cell immunodominance to viruses. Nat Immunol *18*, 456-463. 10.1038/ni.3680.

93. Carbonetti, S., Oliver, B.G., Vigdorovich, V., Dambrauskas, N., Sack, B., Bergl, E., Kappe, S.H.I., and Sather, D.N. (2017). A method for the isolation and characterization of functional murine monoclonal antibodies by single B cell cloning. J Immunol Methods *448*, 66-73. 10.1016/j.jim.2017.05.010.

94. Cornec, D., Berti, A., Hummel, A., Peikert, T., Pers, J.O., and Specks, U. (2017). Identification and phenotyping of circulating autoreactive proteinase 3-specific B cells in patients with PR3-ANCA associated vasculitis and healthy controls. J Autoimmun *84*, 122-131. 10.1016/j.jaut.2017.08.006.

95. Frosch, A.E., Odumade, O.A., Taylor, J.J., Ireland, K., Ayodo, G., Ondigo, B., Narum, D.L., Vulule, J., and John, C.C. (2017). Decrease in Numbers of Naive and Resting B Cells in HIV-Infected Kenyan Adults Leads to a Proportional Increase in Total and Plasmodium falciparum-Specific Atypical Memory B Cells. J Immunol *198*, 4629-4638. 10.4049/jimmunol.1600773.

96. Jimenez-Saiz, R., Chu, D.K., Mandur, T.S., Walker, T.D., Gordon, M.E., Chaudhary, R., Koenig, J., Saliba, S., Galipeau, H.J., Utley, A., King, I.L., Lee, K., Ettinger, R., Waserman, S., Kolbeck, R., and Jordana, M. (2017). Lifelong memory responses perpetuate humoral TH2 immunity and anaphylaxis in food allergy. J Allergy Clin Immunol *140*, 1604-1615 e1605. 10.1016/j.jaci.2017.01.018.

97. Martinez-Murillo, P., Tran, K., Guenaga, J., Lindgren, G., Adori, M., Feng, Y., Phad, G.E., Vazquez Bernat, N., Bale, S., Ingale, J., Dubrovskaya, V., O'Dell, S., Pramanik, L., Spangberg, M., Corcoran, M., Lore, K., Mascola, J.R., Wyatt, R.T., and Karlsson Hedestam, G.B. (2017). Particulate Array of Well-Ordered HIV Clade C Env Trimers Elicits Neutralizing Antibodies that Display a Unique V2 Cap Approach. Immunity *46*, 804-817 e807. 10.1016/j.immuni.2017.04.021.

98. Nair, N., Feng, N., Blum, L.K., Sanyal, M., Ding, S., Jiang, B., Sen, A., Morton, J.M., He, X.S., Robinson, W.H., and Greenberg, H.B. (2017). VP4- and VP7-specific antibodies mediate heterotypic immunity to rotavirus in humans. Sci Transl Med *9*. 10.1126/scitranslmed.aam5434.

99. Ouisse, L.H., Gautreau-Rolland, L., Devilder, M.C., Osborn, M., Moyon, M., Visentin, J., Halary, F., Bruggemann, M., Buelow, R., Anegon, I., and Saulquin, X. (2017). Antigen-specific single B cell sorting and expression-cloning from immunoglobulin humanized rats: a rapid and versatile method for the generation of high affinity and discriminative human monoclonal antibodies. BMC Biotechnol *17*, 3. 10.1186/s12896-016-0322-5.

100. Pinder, C.L., Kratochvil, S., Cizmeci, D., Muir, L., Guo, Y., Shattock, R.J., and McKay, P.F. (2017). Isolation and Characterization of Antigen-Specific Plasmablasts Using a Novel Flow Cytometry-Based Ig Capture Assay. J Immunol *199*, 4180-4188. 10.4049/jimmunol.1701253.

101. Wennhold, K., Thelen, M., Schlosser, H.A., Haustein, N., Reuter, S., Garcia-Marquez, M., Lechner, A., Kobold, S., Rataj, F., Utermohlen, O., Chakupurakal, G., Theurich, S., Hallek, M., Abken, H., Shimabukuro-Vornhagen, A., and von Bergwelt-Baildon, M. (2017). Using Antigen-Specific B Cells to Combine Antibody and T Cell-Based Cancer Immunotherapy. Cancer Immunol Res *5*, 730-743. 10.1158/2326-6066.CIR-16-0236.

102. Wimmers, F., de Haas, N., Scholzen, A., Schreibelt, G., Simonetti, E., Eleveld, M.J., Brouwers, H.M., Beldhuis-Valkis, M., Joosten, I., de Jonge, M.I., Gerritsen, W.R., de Vries, I.J., Diavatopoulos, D.A., and Jacobs, J.F. (2017). Monitoring of dynamic changes in Keyhole Limpet Hemocyanin (KLH)-specific B cells in KLH-vaccinated cancer patients. Sci Rep *7*, 43486. 10.1038/srep43486.

103. Brooks, J.F., Liu, X., Davies, J.M., Wells, J.W., and Steptoe, R.J. (2018). Tetramer-based identification of naive antigen-specific B cells

within a polyclonal repertoire. Eur J Immunol *48*, 1251-1254. 10.1002/eji.201747447.

104. Burton, A.R., Pallett, L.J., McCoy, L.E., Suveizdyte, K., Amin, O.E., Swadling, L., Alberts, E., Davidson, B.R., Kennedy, P.T., Gill, U.S., Mauri, C., Blair, P.A., Pelletier, N., and Maini, M.K. (2018). Circulating and intrahepatic antiviral B cells are defective in hepatitis B. J Clin Invest *128*, 4588-4603. 10.1172/JCI121960.

105. Correa, I., Ilieva, K.M., Crescioli, S., Lombardi, S., Figini, M., Cheung, A., Spicer, J.F., Tutt, A.N.J., Nestle, F.O., Karagiannis, P., Lacy, K.E., and Karagiannis, S.N. (2018). Evaluation of Antigen-Conjugated Fluorescent Beads to Identify Antigen-Specific B Cells. Front Immunol *9*, 493. 10.3389/fimmu.2018.00493.

106. Giesecke, C., Meyer, T., Durek, P., Maul, J., Preiss, J., Jacobs, J.F.M., Thiel, A., Radbruch, A., Ullrich, R., and Dorner, T. (2018). Simultaneous Presence of Non- and Highly Mutated Keyhole Limpet Hemocyanin (KLH)-Specific Plasmablasts Early after Primary KLH Immunization Suggests Cross-Reactive Memory B Cell Activation. J Immunol *200*, 3981-3992. 10.4049/jimmunol.1701728.

107. Hahn, W.O., Butler, N.S., Lindner, S.E., Akilesh, H.M., Sather, D.N., Kappe, S.H., Hamerman, J.A., Gale, M., Jr., Liles, W.C., and Pepper, M. (2018). cGAS-mediated control of blood-stage malaria promotes Plasmodium-specific germinal center responses. JCI Insight *3*. 10.1172/jci.insight.94142.

108. Havenar-Daughton, C., Sarkar, A., Kulp, D.W., Toy, L., Hu, X., Deresa, I., Kalyuzhniy, O., Kaushik, K., Upadhyay, A.A., Menis, S., Landais, E., Cao, L., Diedrich, J.K., Kumar, S., Schiffner, T., Reiss, S.M., Seumois, G., Yates, J.R., Paulson, J.C., Bosinger, S.E., Wilson, I.A., Schief, W.R., and Crotty, S. (2018). The human naive B cell repertoire contains distinct subclasses for a germline-targeting HIV-1 vaccine immunogen. Sci Transl Med *10*. 10.1126/scitranslmed.aat0381.

109. Murugan, R., Buchauer, L., Triller, G., Kreschel, C., Costa, G., Pidelaserra Marti, G., Imkeller, K., Busse, C.E., Chakravarty, S., Sim, B.K.L., Hoffman, S.L., Levashina, E.A., Kremsner, P.G., Mordmuller, B., Hofer, T., and Wardemann, H. (2018). Clonal selection drives protective memory B cell responses in controlled human malaria infection. Sci Immunol *3*. 10.1126/sciimmunol.aap8029.

110. Pape, K.A., Maul, R.W., Dileepan, T., Paustian, A.S., Gearhart, P.J., and Jenkins, M.K. (2018). Naive B Cells with High-Avidity Germline-Encoded Antigen Receptors Produce Persistent IgM(+) and Transient IgG(+) Memory B Cells. Immunity *48*, 1135-1143 e1134. 10.1016/j.immuni.2018.04.019.

111. Rahe, M.C., Gustafson, K.L., and Murtaugh, M.P. (2018). B Cell Tetramer Development for Veterinary Vaccinology. Viral Immunol *31*, 1-10. 10.1089/vim.2017.0073.

112. Scherer, E.M., Smith, R.A., Carter, J.J., Wipf, G.C., Gallego, D.F., Stern, M., Wald, A., and Galloway, D.A. (2018). Analysis of Memory B-Cell Responses Reveals Suboptimal Dosing Schedule of a Licensed Vaccine. J Infect Dis *217*, 572-580. 10.1093/infdis/jix566.

113. Snijder, J., Ortego, M.S., Weidle, C., Stuart, A.B., Gray, M.D., McElrath, M.J., Pancera, M., Veesler, D., and McGuire, A.T. (2018). An Antibody Targeting the Fusion Machinery Neutralizes Dual-Tropic Infection and Defines a Site of Vulnerability on Epstein-Barr Virus. Immunity *48*, 799-811 e799. 10.1016/j.immuni.2018.03.026.

114. Titcombe, P.J., Wigerblad, G., Sippl, N., Zhang, N., Shmagel, A.K., Sahlstrom, P., Zhang, Y., Barsness, L.O., Ghodke-Puranik, Y., Baharpoor, A., Hansson, M., Israelsson, L., Skriner, K., Niewold, T.B., Klareskog, L., Svensson, C.I., Amara, K., Malmstrom, V., and Mueller, D.L. (2018). Pathogenic Citrulline-Multispecific B Cell Receptor Clades in Rheumatoid Arthritis. Arthritis Rheumatol *70*, 1933-1945. 10.1002/art.40590.

115. Allie, S.R., Bradley, J.E., Mudunuru, U., Schultz, M.D., Graf, B.A., Lund, F.E., and Randall, T.D. (2019). The establishment of resident memory B cells in the lung requires local antigen encounter. Nat Immunol *20*, 97-108. 10.1038/s41590-018-0260-6.

116. Bancroft, T., DeBuysscher, B.L., Weidle, C., Schwartz, A., Wall, A., Gray, M.D., Feng, J., Steach, H.R., Fitzpatrick, K.S., Gewe, M.M., Skog, P.D., Doyle-Cooper, C., Ota, T., Strong, R.K., Nemazee, D., Pancera, M., Stamatatos, L., McGuire, A.T., and Taylor, J.J. (2019). Detection and activation of HIV broadly neutralizing antibody precursor B cells using anti-idiotypes. J Exp Med. 10.1084/jem.20190164.

117. Boonpiyathad, T., van de Veen, W., Wirz, O., Sokolowska, M., Ruckert, B., Tan, G., Sangasapaviliya, A., Pradubpongsa, P., Fuengthong, R., Thantiworasit, P., Sirivichayakul, S., Ruxrungtham, K., Akdis, C.A., and Akdis, M. (2019). Role of Der p 1-specific B cells in immune tolerance during 2 years of house dust mite-specific immunotherapy. J Allergy Clin Immunol *143*, 1077-1086 e1010. 10.1016/j.jaci.2018.10.061.

118. Devilder, M.C., Moyon, M., Gautreau-Rolland, L., Navet, B., Perroteau, J., Delbos, F., Gesnel, M.C., Breathnach, R., and Saulquin, X. (2019). Ex vivo evolution of human antibodies by CRISPR-X: from a naive B cell repertoire to affinity matured antibodies. BMC Biotechnol *19*, 14. 10.1186/s12896-019-0504-z.

119. Espeli, M., Bashford-Rogers, R., Sowerby, J.M., Alouche, N., Wong, L., Denton, A.E., Linterman, M.A., and Smith, K.G.C. (2019). FcgammaRIIb differentially regulates pre-immune and germinal center B cell tolerance in mouse and human. Nat Commun *10*, 1970. 10.1038/s41467-019-09434-0.

120. Gatto, M., Wiedemann, A., Nomovi, N., Reiter, K., Schrezenmeier, E., Rose, T., Szelinski, F., Lino, A.C., Valentino, S., Ghirardello, A., Dorner, T., and Doria, A. (2019). Circulating Pentraxin3-Specific B Cells Are Decreased in Lupus Nephritis. Front Immunol *10*, 29. 10.3389/fimmu.2019.00029.

121. Guthmiller, J.J., Dugan, H.L., Neu, K.E., Lan, L.Y., and Wilson, P.C. (2019). An Efficient Method to Generate Monoclonal Antibodies from Human B Cells. Methods Mol Biol *1904*, 109-145. 10.1007/978-1-4939-8958-4_5.

122. Hartweger, H., McGuire, A.T., Horning, M., Taylor, J.J., Dosenovic, P., Yost, D., Gazumyan, A., Seaman, M.S., Stamatatos, L., Jankovic, M., and Nussenzweig, M.C. (2019). HIV-specific humoral immune responses by CRISPR/Cas9-edited B cells. J Exp Med *216*, 1301-1310. 10.1084/jem.20190287.

123. Jimenez-Saiz, R., Ellenbogen, Y., Koenig, J.F.E., Gordon, M.E., Walker, T.D., Rosace, D., Spill, P., Bruton, K., Kong, J., Monteiro, K., Wen, J., Tuomanen, E.I., Kolbeck, R., Chu, D.K., Waserman, S., and Jordana, M. (2019). IgG1(+) B-cell immunity predates IgE responses in epicutaneous sensitization to foods. Allergy *74*, 165-175. 10.1111/all.13481.

124. Li, K., Wang, S., Cao, Y., Bao, H., Li, P., Sun, P., Bai, X., Fu, Y., Ma, X., Zhang, J., Li, D., Chen, Y., Liu, X., An, F., Wu, F., Lu, Z., and Liu, Z. (2019). Development of Foot-and-Mouth Disease Virus-Neutralizing Monoclonal Antibodies Derived From Plasmablasts of Infected Cattle and Their Germline Gene Usage. Front Immunol *10*, 2870. 10.3389/fimmu.2019.02870.

125. Martinov, T., Swanson, L.A., Breed, E.R., Tucker, C.G., Dwyer, A.J., Johnson, J.K., Mitchell, J.S., Sahli, N.L., Wilson, J.C., Singh, L.M., Hogquist, K.A., Spanier, J.A., and Fife, B.T. (2019).

Programmed Death-1 Restrains the Germinal Center in Type 1 Diabetes. J Immunol *203*, 844-852. 10.4049/jimmunol.1801535.

126. Moffett, H.F., Harms, C.K., Fitzpatrick, K.S., Tooley, M.R., Boonyaratanakornkit, J., and Taylor, J.J. (2019). B cells engineered to express pathogen-specific antibodies protect against infection. Sci Immunol *4*. 10.1126/sciimmunol.aax0644.

127. Price, M.J., Hicks, S.L., Bradley, J.E., Randall, T.D., Boss, J.M., and Scharer, C.D. (2019). IgM, IgG, and IgA Influenza-Specific Plasma Cells Express Divergent Transcriptomes. J Immunol *203*, 2121-2129. 10.4049/jimmunol.1900285.

128. Roco, J.A., Mesin, L., Binder, S.C., Nefzger, C., Gonzalez-Figueroa, P., Canete, P.F., Ellyard, J., Shen, Q., Robert, P.A., Cappello, J., Vohra, H., Zhang, Y., Nowosad, C.R., Schiepers, A., Corcoran, L.M., Toellner, K.M., Polo, J.M., Meyer-Hermann, M., Victora, G.D., and Vinuesa, C.G. (2019). Class-Switch Recombination Occurs Infrequently in Germinal Centers. Immunity *51*, 337-350 e337. 10.1016/j.immuni.2019.07.001.

129. Sangesland, M., Ronsard, L., Kazer, S.W., Bals, J., Boyoglu-Barnum, S., Yousif, A.S., Barnes, R., Feldman, J., Quirindongo-Crespo, M., McTamney, P.M., Rohrer, D., Lonberg, N., Chackerian, B., Graham, B.S., Kanekiyo, M., Shalek, A.K., and Lingwood, D. (2019). Germline-Encoded Affinity for Cognate Antigen Enables Vaccine Amplification of a Human Broadly Neutralizing Response against Influenza Virus. Immunity *51*, 735-749 e738. 10.1016/j.immuni.2019.09.001.

130. Schlosser, H.A., Thelen, M., Lechner, A., Wennhold, K., Garcia-Marquez, M.A., Rothschild, S.I., Staib, E., Zander, T., Beutner, D., Gathof, B., Gilles, R., Cukuroglu, E., Goke, J., Shimabukuro-Vornhagen, A., Drebber, U., Quaas, A., Bruns, C.J., Holscher, A.H., and Von Bergwelt-Baildon, M.S. (2019). B cells in esophago-gastric adenocarcinoma are highly differentiated, organize in tertiary lymphoid structures and produce tumor-specific antibodies. Oncoimmunology *8*, e1512458. 10.1080/2162402X.2018.1512458.

131. Setliff, I., Shiakolas, A.R., Pilewski, K.A., Murji, A.A., Mapengo, R.E., Janowska, K., Richardson, S., Oosthuysen, C., Raju, N., Ronsard, L., Kanekiyo, M., Qin, J.S., Kramer, K.J., Greenplate, A.R., McDonnell, W.J., Graham, B.S., Connors, M., Lingwood, D., Acharya, P., Morris, L., and Georgiev, I.S. (2019). High-Throughput Mapping of B Cell Receptor Sequences to Antigen Specificity. Cell *179*, 1636-1646 e1615. 10.1016/j.cell.2019.11.003.

132. Takata, K., Stathopoulos, P., Cao, M., Mane-Damas, M., Fichtner, M.L., Benotti, E.S., Jacobson, L., Waters, P., Irani, S.R., Martinez-Martinez, P., Beeson, D., Losen, M., Vincent, A., Nowak, R.J., and O'Connor, K.C. (2019). Characterization of pathogenic monoclonal autoantibodies derived from muscle-specific kinase myasthenia gravis patients. JCI Insight *4*. 10.1172/jci.insight.127167.

133. Voss, J.E., Gonzalez-Martin, A., Andrabi, R., Fuller, R.P., Murrell, B., McCoy, L.E., Porter, K., Huang, D., Li, W., Sok, D., Le, K., Briney, B., Chateau, M., Rogers, G., Hangartner, L., Feeney, A.J., Nemazee, D., Cannon, P., and Burton, D.R. (2019). Reprogramming the antigen specificity of B cells using genome-editing technologies. Elife *8*. 10.7554/eLife.42995.

134. Agazio, A., Cimons, J., Shotts, K.M., Guo, K., Santiago, M.L., Pelanda, R., and Torres, R.M. (2020). Histone H2A-Reactive B Cells Are Functionally Anergic in Healthy Mice With Potential to Provide Humoral Protection Against HIV-1. Front Immunol *11*, 1565. 10.3389/fimmu.2020.01565.

135. Alterauge, D., Bagnoli, J.W., Dahlstrom, F., Bradford, B.M., Mabbott, N.A., Buch, T., Enard, W., and Baumjohann, D. (2020). Continued Bcl6 Expression Prevents the Transdifferentiation of Established Tfh Cells into Th1 Cells during Acute Viral Infection. Cell Rep *33*, 108232. 10.1016/j.celrep.2020.108232.

136. Aye, R., Sutton, H.J., Nduati, E.W., Kai, O., Mwacharo, J., Musyoki, J., Otieno, E., Wambua, J., Bejon, P., Cockburn, I.A., and Ndungu, F.M. (2020). Malaria exposure drives both cognate and bystander human B cells to adopt an atypical phenotype. Eur J Immunol *50*, 1187-1194. 10.1002/eji.201948473.

137. Brooks, J.F., Murphy, P.R., Barber, J.E.M., Wells, J.W., and Steptoe, R.J. (2020). Peripheral Tolerance Checkpoints Imposed by Ubiquitous Antigen Expression Limit Antigen-Specific B Cell Responses under Strongly Immunogenic Conditions. J Immunol *205*, 1239-1247. 10.4049/jimmunol.2000377.

138. Carnathan, D.G., Kaushik, K., Ellebedy, A.H., Enemuo, C.A., Gebru, E.H., Dhadvai, P., Rasheed, M.A.U., Pauthner, M.G., Ozorowski, G., Ahmed, R., Burton, D.R., Ward, A.B., Silvestri, G., Crotty, S., and Locci, M. (2020). Harnessing Activin A Adjuvanticity to Promote Antibody Responses to BG505 HIV Envelope Trimers. Front Immunol *11*, 1213. 10.3389/fimmu.2020.01213.

139. Coelho, C.H., Nadakal, S.T., Gonzales Hurtado, P., Morrison, R., Galson, J.D., Neal, J., Wu, Y., King, C.R., Price, V., Miura, K., Wong-Madden, S., Alamou Doritchamou, J.Y., Narum, D.L., MacDonald, N.J., Snow-Smith, M., Vignali, M., Taylor, J.J., Lefranc, M.P., Truck, J., Long, C.A., Sagara, I., Fried, M., and Duffy, P.E. (2020). Antimalarial antibody repertoire defined by plasma IG proteomics and single B cell IG sequencing. JCI Insight *5*. 10.1172/jci.insight.143471.

140. Godot, V., Tcherakian, C., Gil, L., Cervera-Marzal, I., Li, G., Cheng, L., Ortonne, N., Lelievre, J.D., Pantaleo, G., Fenwick, C., Centlivre, M., Mouquet, H., Cardinaud, S., Zurawski, S.M., Zurawski, G., Milpied, P., Su, L., and Levy, Y. (2020). TLR-9 agonist and CD40-targeting vaccination induces HIV-1 envelope-specific B cells with a diversified immunoglobulin repertoire in humanized mice. PLoS Pathog *16*, e1009025. 10.1371/journal.ppat.1009025.

141. Huang, D., Tran, J.T., Olson, A., Vollbrecht, T., Guryleva, M.V., Tenuta, M., Fuller, R.P., Schiffner, T., Abadejos, J.R., Couvrette, L., Blane, T.R., Saye, K., Li, W., Landais, E., Gonzalez-Martin, A., Schief, W., Murrell, B., Burton, D.R., Nemazee, D., and Voss, J.E. (2020). Vaccine Elicitation of HIV Broadly Neutralizing Antibodies from Engineered B cells. bioRxiv, 2020.2003.2017.989699. 10.1101/2020.03.17.989699.

142. Johnson, J.L., Rosenthal, R.L., Knox, J.J., Myles, A., Naradikian, M.S., Madej, J., Kostiv, M., Rosenfeld, A.M., Meng, W., Christensen, S.R., Hensley, S.E., Yewdell, J., Canaday, D.H., Zhu, J., McDermott, A.B., Dori, Y., Itkin, M., Wherry, E.J., Pardi, N., Weissman, D., Naji, A., Prak, E.T.L., Betts, M.R., and Cancro, M.P. (2020). The Transcription Factor T-bet Resolves Memory B Cell Subsets with Distinct Tissue Distributions and Antibody Specificities in Mice and Humans. Immunity *52*, 842-855 e846. 10.1016/j.immuni.2020.03.020.

143. Kealy, L., Di Pietro, A., Hailes, L., Scheer, S., Dalit, L., Groom, J.R., Zaph, C., and Good-Jacobson, K.L. (2020). The Histone Methyltransferase DOT1L Is Essential for Humoral Immune Responses. Cell Rep *33*, 108504. 10.1016/j.celrep.2020.108504.

144. Khiew, S.H., Jain, D., Chen, J., Yang, J., Yin, D., Young, J.S., Dent, A., Sciammas, R., Alegre, M.L., and Chong, A.S. (2020). Transplantation tolerance modifies donor-specific B cell fate to suppress de novo alloreactive B cells. J Clin Invest *130*, 3453-3466. 10.1172/JCI132814.

145. Kramer, C.S.M., Franke-van Dijk, M.E.I., Bakker, K.H., Uyar-Mercankaya, M., Karahan, G.E., Roelen, D.L., Claas, F.H.J., and Heidt, S. (2020). Generation and reactivity analysis of human recombinant monoclonal antibodies directed against epitopes on HLA-DR. Am J Transplant *20*, 3341-3353. 10.1111/ajt.15950.

146. Kristyanto, H., Blomberg, N.J., Slot, L.M., van der Voort, E.I.H., Kerkman, P.F., Bakker, A., Burgers, L.E., Ten Brinck, R.M., van der Helm-van Mil, A.H.M., Spits, H., Baeten, D.L., Huizinga, T.W.J., Toes, R.E.M., and Scherer, H.U. (2020). Persistently activated, proliferative memory autoreactive B cells promote inflammation in rheumatoid arthritis. Sci Transl Med *12*. 10.1126/scitranslmed.aaz5327.

147. Kunzli, M., Schreiner, D., Pereboom, T.C., Swarnalekha, N., Litzler, L.C., Lotscher, J., Ertuna, Y.I., Roux, J., Geier, F., Jakob, R.P., Maier, T., Hess, C., Taylor, J.J., and King, C.G. (2020). Long-lived T follicular helper cells retain plasticity and help sustain humoral immunity. Sci Immunol *5*. 10.1126/sciimmunol.aay5552.

148. Lederer, K., Castano, D., Gomez Atria, D., Oguin, T.H., 3rd, Wang, S., Manzoni, T.B., Muramatsu, H., Hogan, M.J., Amanat, F., Cherubin, P., Lundgreen, K.A., Tam, Y.K., Fan, S.H.Y., Eisenlohr, L.C., Maillard, I., Weissman, D., Bates, P., Krammer, F., Sempowski, G.D., Pardi, N., and Locci, M. (2020). SARS-CoV-2 mRNA Vaccines Foster Potent Antigen-Specific Germinal Center Responses Associated with Neutralizing Antibody Generation. Immunity *53*, 1281-1295 e1285. 10.1016/j.immuni.2020.11.009.

149. Mesin, L., Schiepers, A., Ersching, J., Barbulescu, A., Cavazzoni, C.B., Angelini, A., Okada, T., Kurosaki, T., and Victora, G.D. (2020). Restricted Clonality and Limited Germinal Center Reentry Characterize Memory B Cell Reactivation by Boosting. Cell *180*, 92-106 e111. 10.1016/j.cell.2019.11.032.

150. Nahmad, A.D., Raviv, Y., Horovitz-Fried, M., Sofer, I., Akriv, T., Nataf, D., Dotan, I., Burstein, D., Wine, Y., Benhar, I., and Barzel, A. (2020). B cells engineered to express an anti-HIV antibody allow memory retention, class switch recombination and clonal selection in mice. bioRxiv, 2020.2002.2028.970822. 10.1101/2020.02.28.970822.

151. Phad, G.E., Pushparaj, P., Tran, K., Dubrovskaya, V., Adori, M., Martinez-Murillo, P., Vazquez Bernat, N., Singh, S., Dionne, G., O'Dell, S., Bhullar, K., Narang, S., Sorini, C., Villablanca, E.J., Sundling, C., Murrell, B., Mascola, J.R., Shapiro, L., Pancera, M., Martin, M., Corcoran, M., Wyatt, R.T., and Karlsson Hedestam, G.B. (2020). Extensive dissemination and intraclonal maturation of HIV Env vaccine-induced B cell responses. J Exp Med *217*. 10.1084/jem.20191155.

152. Steach, H.R., DeBuysscher, B.L., Schwartz, A., Boonyaratanakornkit, J., Baker, M.L., Tooley, M.R., Pease, N.A., and Taylor, J.J. (2020). Cross-Reactivity with Self-Antigen Tunes the Functional Potential of Naive B Cells Specific for Foreign Antigens. J Immunol *204*, 498-509. 10.4049/jimmunol.1900799.

153. Wec, A.Z., Haslwanter, D., Abdiche, Y.N., Shehata, L., Pedreno-Lopez, N., Moyer, C.L., Bornholdt, Z.A., Lilov, A., Nett, J.H., Jangra, R.K., Brown, M., Watkins, D.I., Ahlm, C., Forsell, M.N., Rey, F.A., Barba-Spaeth, G., Chandran, K., and Walker, L.M. (2020). Longitudinal dynamics of the human B cell response to the yellow fever 17D vaccine. Proc Natl Acad Sci U S A *117*, 6675-6685. 10.1073/pnas.1921388117.

154. Wec, A.Z., Wrapp, D., Herbert, A.S., Maurer, D.P., Haslwanter, D., Sakharkar, M., Jangra, R.K., Dieterle, M.E., Lilov, A., Huang, D., Tse, L.V., Johnson, N.V., Hsieh, C.L., Wang, N., Nett, J.H., Champney, E., Burnina, I., Brown, M., Lin, S., Sinclair, M., Johnson, C., Pudi, S., Bortz, R., 3rd, Wirchnianski, A.S., Laudermilch, E., Florez, C., Fels, J.M., O'Brien, C.M., Graham, B.S., Nemazee, D., Burton, D.R., Baric, R.S., Voss, J.E., Chandran, K., Dye, J.M., McLellan, J.S., and Walker, L.M. (2020). Broad neutralization of SARS-related viruses by human monoclonal antibodies. Science *369*, 731-736. 10.1126/science.abc7424.

155. Wong, R., Belk, J.A., Govero, J., Uhrlaub, J.L., Reinartz, D., Zhao, H., Errico, J.M., D'Souza, L., Ripperger, T.J., Nikolich-Zugich, J., Shlomchik, M.J., Satpathy, A.T., Fremont, D.H., Diamond, M.S., and Bhattacharya, D. (2020). Affinity-Restricted Memory B Cells Dominate Recall Responses to Heterologous Flaviviruses. Immunity *53*, 1078-1094 e1077. 10.1016/j.immuni.2020.09.001.

156. Wong, R., and Bhattacharya, D. (2020). ZBTB38 is dispensable for antibody responses. PLoS One *15*, e0235183. 10.1371/journal.pone.0235183.

157. Al Qureshah, F., Sagadiev, S., Thouvenel, C.D., Liu, S., Hua, Z., Hou, B., Acharya, M., James, R.G., and Rawlings, D.J. (2021). Activated PI3Kdelta signals compromise plasma cell survival via limiting autophagy and increasing ER stress. J Exp Med *218*. 10.1084/jem.20211035.

158. Alameh, M.G., Tombacz, I., Bettini, E., Lederer, K., Sittplangkoon, C., Wilmore, J.R., Gaudette, B.T., Soliman, O.Y., Pine, M., Hicks, P., Manzoni, T.B., Knox, J.J., Johnson, J.L., Laczko, D., Muramatsu, H., Davis, B., Meng, W., Rosenfeld, A.M., Strohmeier, S., Lin, P.J.C., Mui, B.L., Tam, Y.K., Kariko, K., Jacquet, A., Krammer, F., Bates, P., Cancro, M.P., Weissman, D., Luning Prak, E.T., Allman, D., Locci, M., and Pardi, N. (2021). Lipid nanoparticles enhance the efficacy of mRNA and protein subunit vaccines by inducing robust T follicular helper cell and humoral responses. Immunity *54*, 2877-2892 e2877. 10.1016/j.immuni.2021.11.001.

159. Awasthi, S., Knox, J.J., Desmond, A., Alameh, M.G., Gaudette, B.T., Lubinski, J.M., Naughton, A., Hook, L.M., Egan, K.P., Tam, Y.K., Pardi, N., Allman, D., Luning Prak, E.T., Cancro, M.P., Weissman, D., Cohen, G.H., and Friedman, H.M. (2021). Trivalent nucleoside-modified mRNA vaccine yields durable memory B cell protection against genital herpes in preclinical models. J Clin Invest *131*. 10.1172/JCI152310.

160. Boonyaratanakornkit, J., Singh, S., Weidle, C., Rodarte, J., Bakthavatsalam, R., Perkins, J., Stewart-Jones, G.B.E., Kwong, P.D., McGuire, A.T., Pancera, M., and Taylor, J.J. (2021). Protective antibodies against human parainfluenza virus type 3 infection. MAbs *13*, 1912884. 10.1080/19420862.2021.1912884.

161. Brooks, J.F., Tan, C., Mueller, J.L., Hibiya, K., Hiwa, R., Vykunta, V., and Zikherman, J. (2021). Negative feedback by NUR77/Nr4a1 restrains B cell clonal dominance during early T-dependent immune responses. Cell Rep *36*, 109645. 10.1016/j.celrep.2021.109645.

162. Byazrova, M., Yusubalieva, G., Spiridonova, A., Efimov, G., Mazurov, D., Baranov, K., Baklaushev, V., and Filatov, A. (2021). Pattern of circulating SARS-CoV-2-specific antibody-secreting and memory B-cell generation in patients with acute COVID-19. Clin Transl Immunology *10*, e1245. 10.1002/cti2.1245.

163. Chatterjee, D., Lewis, F.J., Sutton, H.J., Kaczmarski, J.A., Gao, X., Cai, Y., McNamara, H.A., Jackson, C.J., and Cockburn, I.A. (2021). Avid binding by B cells to the Plasmodium circumsporozoite protein repeat suppresses responses to protective subdominant epitopes. Cell Rep *35*, 108996. 10.1016/j.celrep.2021.108996.

164. Cheon, I.S., Li, C., Son, Y.M., Goplen, N.P., Wu, Y., Cassmann, T., Wang, Z., Wei, X., Tang, J., Li, Y., Marlow, H., Hughes, S., Hammel, L., Cox, T.M., Goddery, E., Ayasoufi, K., Weiskopf, D., Boonyaratanakornkit, J., Dong, H., Li, H., Chakraborty, R., Johnson, A.J., Edell, E., Taylor, J.J., Kaplan, M.H., Sette, A., Bartholmai, B.J., Kern, R., Vassallo, R., and Sun, J. (2021). Immune signatures underlying post-acute COVID-19 lung sequelae. Sci Immunol *6*, eabk1741. 10.1126/sciimmunol.abk1741.

165. Coelho, C.H., Galson, J.D., Truck, J., and Duffy, P.E. (2021). B cell clonal expansion and mutation in the immunoglobulin heavy chain variable domain in response to Pfs230 and Pfs25 malaria vaccines. Int J Parasitol. 10.1016/j.ijpara.2021.11.008.

166. Coelho, C.H., Tang, W.K., Burkhardt, M., Galson, J.D., Muratova, O., Salinas, N.D., Alves, E.S.T.L., Reiter, K., MacDonald, N.J., Nguyen, V., Herrera, R., Shimp, R., Narum, D.L., Byrne-Steele, M., Pan, W., Hou, X., Brown, B., Eisenhower, M., Han, J., Jenkins, B.J., Doritchamou, J.Y.A., Smelkinson, M.G., Vega-Rodriguez, J., Truck, J., Taylor, J.J., Sagara, I., Healy, S.A., Renn, J.P., Tolia, N.H., and Duffy, P.E. (2021). A human monoclonal antibody blocks malaria transmission and defines a highly conserved neutralizing epitope on gametes. Nat Commun *12*, 1750. 10.1038/s41467-021-21955-1.

167. Cossarizza, A., Chang, H.D., Radbruch, A., Abrignani, S., Addo, R., Akdis, M., Andra, I., Andreata, F., Annunziato, F., Arranz, E., Bacher, P., Bari, S., Barnaba, V., Barros-Martins, J., Baumjohann, D., Beccaria, C.G., Bernardo, D., Boardman, D.A., Borger, J., Bottcher, C., Brockmann, L., Burns, M., Busch, D.H., Cameron, G., Cammarata, I., Cassotta, A., Chang, Y., Chirdo, F.G., Christakou, E., Cicin-Sain, L., Cook, L., Corbett, A.J., Cornelis, R., Cosmi, L., Davey, M.S., De Biasi, S., De Simone, G., Del Zotto, G., Delacher, M., Di Rosa, F., Di Santo, J., Diefenbach, A., Dong, J., Dorner, T., Dress, R.J., Dutertre, C.A., Eckle, S.B.G., Eede, P., Evrard, M., Falk, C.S., Feuerer, M., Fillatreau, S., Fiz-Lopez, A., Follo, M., Foulds, G.A., Frobel, J., Gagliani, N., Galletti, G., Gangaev, A., Garbi, N., Garrote, J.A., Geginat, J., Gherardin, N.A., Gibellini, L., Ginhoux, F., Godfrey, D.I., Gruarin, P., Haftmann, C., Hansmann, L., Harpur, C.M., Hayday, A.C., Heine, G., Hernandez, D.C., Herrmann, M., Hoelsken, O., Huang, Q., Huber, S., Huber, J.E., Huehn, J., Hundemer, M., Hwang, W.Y.K., Iannacone, M., Ivison, S.M., Jack, H.M., Jani, P.K., Keller, B., Kessler, N., Ketelaars, S., Knop, L., Knopf, J., Koay, H.F., Kobow, K., Kriegsmann, K., Kristyanto, H., Krueger, A., Kuehne, J.F., Kunze-Schumacher, H., Kvistborg, P., Kwok, I., Latorre, D., Lenz, D., Levings, M.K., Lino, A.C., Liotta, F., Long, H.M., Lugli, E., MacDonald, K.N., Maggi, L., Maini, M.K., Mair, F., Manta, C., Manz, R.A., Mashreghi, M.F., Mazzoni, A., McCluskey, J., Mei, H.E., Melchers, F., Melzer, S., Mielenz, D., Monin, L., Moretta, L., Multhoff, G., Munoz, L.E., Munoz-Ruiz, M., Muscate, F., Natalini, A., Neumann, K., Ng, L.G., Niedobitek, A., Niemz, J., Almeida, L.N., Notarbartolo, S., Ostendorf, L., Pallett, L.J., Patel, A.A., Percin, G.I., Peruzzi, G., Pinti, M., Pockley, A.G., Pracht, K., Prinz, I., Pujol-Autonell, I., Pulvirenti, N., Quatrini, L., Quinn, K.M., Radbruch, H., Rhys, H., Rodrigo, M.B., Romagnani, C., Saggau, C., Sakaguchi, S., Sallusto, F., Sanderink, L., Sandrock, I., Schauer, C., Scheffold, A., Scherer, H.U., Schiemann, M., Schildberg, F.A., Schober, K., Schoen, J., Schuh, W., Schuler, T., Schulz, A.R., Schulz, S., Schulze, J., Simonetti, S., Singh, J., Sitnik, K.M., Stark, R., Starossom, S., Stehle, C., Szelinski, F., Tan, L., Tarnok, A., Tornack, J., Tree, T.I.M., van Beek, J.J.P., van de Veen, W., van Gisbergen, K., Vasco, C., Verheyden, N.A., von Borstel, A., Ward-Hartstonge, K.A., Warnatz, K., Waskow, C., Wiedemann, A., Wilharm, A., Wing, J., Wirz, O., Wittner, J., Yang, J.H.M., and Yang, J. (2021). Guidelines for the use of flow cytometry and cell sorting in immunological studies (third edition). Eur J Immunol *51*, 2708-3145. 10.1002/eji.202170126.

168. Dan, J.M., Mateus, J., Kato, Y., Hastie, K.M., Yu, E.D., Faliti, C.E., Grifoni, A., Ramirez, S.I., Haupt, S., Frazier, A., Nakao, C., Rayaprolu, V., Rawlings, S.A., Peters, B., Krammer, F., Simon, V., Saphire, E.O., Smith, D.M., Weiskopf, D., Sette, A., and Crotty, S. (2021). Immunological memory to SARS-CoV-2 assessed for up to 8 months after infection. Science *371*. 10.1126/science.abf4063.

169. Duan, L., Liu, D., Chen, H., Mintz, M.A., Chou, M.Y., Kotov, D.I., Xu, Y., An, J., Laidlaw, B.J., and Cyster, J.G. (2021). Follicular dendritic cells restrict interleukin-4 availability in germinal centers and foster memory B cell generation. Immunity *54*, 2256-2272 e2256. 10.1016/j.immuni.2021.08.028.

170. Dugan, H.L., Stamper, C.T., Li, L., Changrob, S., Asby, N.W., Halfmann, P.J., Zheng, N.Y., Huang, M., Shaw, D.G., Cobb, M.S., Erickson, S.A., Guthmiller, J.J., Stovicek, O., Wang, J., Winkler, E.S., Madariaga, M.L., Shanmugarajah, K., Jansen, M.O., Amanat, F., Stewart, I., Utset, H.A., Huang, J., Nelson, C.A., Dai, Y.N., Hall, P.D., Jedrzejczak, R.P., Joachimiak, A., Krammer, F., Diamond, M.S., Fremont, D.H., Kawaoka, Y., and Wilson, P.C. (2021). Profiling B cell immunodominance after SARS-CoV-2 infection reveals antibody evolution to non-neutralizing viral targets. Immunity *54*, 1290-1303 e1297. 10.1016/j.immuni.2021.05.001.

171. Feldman, J., Bals, J., Altomare, C.G., St Denis, K., Lam, E.C., Hauser, B.M., Ronsard, L., Sangesland, M., Moreno, T.B., Okonkwo, V., Hartojo, N., Balazs, A.B., Bajic, G., Lingwood, D., and Schmidt, A.G. (2021). Naive human B cells engage the receptor binding domain of SARS-CoV-2, variants of concern, and related sarbecoviruses. Sci Immunol *6*, eabl5842. 10.1126/sciimmunol.abl5842.

172. Goel, R.R., Painter, M.M., Apostolidis, S.A., Mathew, D., Meng, W., Rosenfeld, A.M., Lundgreen, K.A., Reynaldi, A., Khoury, D.S., Pattekar, A., Gouma, S., Kuri-Cervantes, L., Hicks, P., Dysinger, S., Hicks, A., Sharma, H., Herring, S., Korte, S., Baxter, A.E., Oldridge, D.A., Giles, J.R., Weirick, M.E., McAllister, C.M., Awofolaju, M., Tanenbaum, N., Drapeau, E.M., Dougherty, J., Long, S., D'Andrea, K., Hamilton, J.T., McLaughlin, M., Williams, J.C., Adamski, S., Kuthuru, O., dagger, U.P.C.P.U., Frank, I., Betts, M.R., Vella, L.A., Grifoni, A., Weiskopf, D., Sette, A., Hensley, S.E., Davenport, M.P., Bates, P., Luning Prak, E.T., Greenplate, A.R., and Wherry, E.J. (2021). mRNA vaccines induce durable immune memory to SARS-CoV-2 and variants of concern. Science *374*, abm0829. 10.1126/science.abm0829.

173. Harrell, J.E., Kurtz, J.R., Bauer, D.L., Prior, J.T., Gellings, P.S., Morici, L.A., and McLachlan, J.B. (2021). An Outer Membrane Vesicle-Adjuvanted Oral Vaccine Protects Against Lethal, Oral Salmonella Infection. Pathogens *10*. 10.3390/pathogens10050616.

174. Hopp, C.S., Sekar, P., Diouf, A., Miura, K., Boswell, K., Skinner, J., Tipton, C.M., Peterson, M.E., Chambers, M.J., Andrews, S., Lu, J., Tan, J., Li, S., Doumbo, S., Kayentao, K., Ongoiba, A., Traore, B., Portugal, S., Sun, P.D., Long, C., Koup, R.A., Long, E.O., McDermott, A.B., and Crompton, P.D. (2021). Plasmodium falciparum-specific IgM B cells dominate in children, expand with malaria, and produce functional IgM. J Exp Med *218*. 10.1084/jem.20200901.

175. Inoue, T., Shinnakasu, R., Kawai, C., Ise, W., Kawakami, E., Sax, N., Oki, T., Kitamura, T., Yamashita, K., Fukuyama, H., and Kurosaki, T. (2021). Exit from germinal center to become quiescent memory B cells depends on metabolic reprograming and provision of a survival signal. J Exp Med *218*. 10.1084/jem.20200866.

176. Pape, K.A., Dileepan, T., Kabage, A.J., Kozysa, D., Batres, R., Evert, C., Matson, M., Lopez, S., Krueger, P.D., Graiziger, C., Vaughn, B.P., Shmidt, E., Rhein, J., Schacker, T.W., Khoruts, A., and Jenkins, M.K. (2021). High-affinity memory B cells induced by SARS-CoV-2 infection produce more plasmablasts and atypical memory B cells than those primed by mRNA vaccines. Cell Rep *37*, 109823. 10.1016/j.celrep.2021.109823.

177. Poon, M.M.L., Rybkina, K., Kato, Y., Kubota, M., Matsumoto, R., Bloom, N.I., Zhang, Z., Hastie, K.M., Grifoni, A., Weiskopf, D., Wells, S.B., Ural, B.B., Lam, N., Szabo, P.A., Dogra, P., Lee, Y.S., Gray, J.I., Bradley, M.C., Brusko, M.A., Brusko, T.M., Saphire, E.O., Connors, T.J., Sette, A., Crotty, S., and Farber, D.L. (2021). SARS-CoV-2 infection generates tissue-localized immunological memory in humans. Sci Immunol *6*, eabl9105. 10.1126/sciimmunol.abl9105.

178. Prior, J.T., Davitt, C., Kurtz, J., Gellings, P., McLachlan, J.B., and Morici, L.A. (2021). Bacterial-Derived Outer Membrane Vesicles are Potent Adjuvants that Drive Humoral and Cellular Immune Responses. Pharmaceutics *13*. 10.3390/pharmaceutics13020131.

179. Radke, E.E., Li, Z., Hernandez, D.N., El Bannoudi, H., Kosakovsky Pond, S.L., Shopsin, B., Lopez, P., Fenyo, D., and Silverman, G.J. (2021). Diversity of Functionally Distinct Clonal Sets of Human Conventional Memory B Cells That Bind Staphylococcal Protein A. Front Immunol *12*, 662782. 10.3389/fimmu.2021.662782.

180. Reyes, R.A., Clarke, K., Gonzales, S.J., Cantwell, A.M., Garza, R., Catano, G., Tragus, R.E., Patterson, T.F., Bol, S., and Bunnik, E.M. (2021). SARS-CoV-2 spike-specific memory B cells express higher levels of T-bet and FcRL5 after non-severe COVID-19 as compared to severe disease. PLoS One *16*, e0261656. 10.1371/journal.pone.0261656.

181. Rincon-Arevalo, H., Choi, M., Stefanski, A.L., Halleck, F., Weber, U., Szelinski, F., Jahrsdorfer, B., Schrezenmeier, H., Ludwig, C., Sattler, A., Kotsch, K., Potekhin, A., Chen, Y., Burmester, G.R., Eckardt, K.U., Guerra, G.M., Durek, P., Heinrich, F., Ferreira-Gomes, M., Radbruch, A., Budde, K., Lino, A.C., Mashreghi, M.F., Schrezenmeier, E., and Dorner, T. (2021). Impaired humoral immunity to SARS-CoV-2 BNT162b2 vaccine in kidney transplant recipients and dialysis patients. Sci Immunol *6*. 10.1126/sciimmunol.abj1031.

182. Rodda, L.B., Netland, J., Shehata, L., Pruner, K.B., Morawski, P.A., Thouvenel, C.D., Takehara, K.K., Eggenberger, J., Hemann, E.A., Waterman, H.R., Fahning, M.L., Chen, Y., Hale, M., Rathe, J., Stokes, C., Wrenn, S., Fiala, B., Carter, L., Hamerman, J.A., King, N.P., Gale, M., Jr., Campbell, D.J., Rawlings, D.J., and Pepper, M. (2021). Functional SARS-CoV-2-Specific Immune Memory Persists after Mild COVID-19. Cell *184*, 169-183 e117. 10.1016/j.cell.2020.11.029.

183. Seydoux, E., Wan, Y.H., Feng, J., Wall, A., Aljedani, S., Homad, L.J., MacCamy, A.J., Weidle, C., Gray, M.D., Brumage, L., Taylor, J.J., Pancera, M., Stamatatos, L., and McGuire, A.T. (2021). Development of a VRC01-class germline targeting immunogen derived from anti-idiotypic antibodies. Cell Rep *35*, 109084. 10.1016/j.celrep.2021.109084.

184. Shroff, R.T., Chalasani, P., Wei, R., Pennington, D., Quirk, G., Schoenle, M.V., Peyton, K.L., Uhrlaub, J.L., Ripperger, T.J., Jergovic, M., Dalgai, S., Wolf, A., Whitmer, R., Hammad, H., Carrier, A., Scott, A.J., Nikolich-Zugich, J., Worobey, M., Sprissler, R., Dake, M., LaFleur, B.J., and Bhattacharya, D. (2021). Immune responses to two and three doses of the BNT162b2 mRNA vaccine in adults with solid tumors. Nat Med *27*, 2002-2011. 10.1038/s41591-021-01542-z.

185. Slot, L.M., Vergroesen, R.D., Kerkman, P.F., Staudinger, E., Reijm, S., van Dooren, H.J., van der Voort, E.I.H., Huizinga, T.W.J., Toes, R.E.M., and Scherer, H.U. (2021). Light chain skewing in autoantibodies and B-cell receptors of the citrullinated antigen-binding B-cell response in rheumatoid arthritis. PLoS One *16*, e0247847. 10.1371/journal.pone.0247847.

186. Son, Y.M., Cheon, I.S., Wu, Y., Li, C., Wang, Z., Gao, X., Chen, Y., Takahashi, Y., Fu, Y.X., Dent, A.L., Kaplan, M.H., Taylor, J.J., Cui, W., and Sun, J. (2021). Tissue-resident CD4(+) T helper cells assist the development of protective respiratory B and CD8(+) T cell memory responses. Sci Immunol *6*. 10.1126/sciimmunol.abb6852.

187. Sutton, H.J., Aye, R., Idris, A.H., Vistein, R., Nduati, E., Kai, O., Mwacharo, J., Li, X., Gao, X., Andrews, T.D., Koutsakos, M., Nguyen, T.H.O., Nekrasov, M., Milburn, P., Eltahla, A., Berry, A.A., Kc, N., Chakravarty, S., Sim, B.K.L., Wheatley, A.K., Kent, S.J., Hoffman, S.L., Lyke, K.E., Bejon, P., Luciani, F., Kedzierska, K., Seder, R.A., Ndungu, F.M., and Cockburn, I.A. (2021). Atypical B cells are part of an alternative lineage of B cells that participates in responses to vaccination and infection in humans. Cell Rep *34*, 108684. 10.1016/j.celrep.2020.108684.

188. Turner, J.S., Kim, W., Kalaidina, E., Goss, C.W., Rauseo, A.M., Schmitz, A.J., Hansen, L., Haile, A., Klebert, M.K., Pusic, I., O'Halloran, J.A., Presti, R.M., and Ellebedy, A.H. (2021). SARS-CoV-2 infection induces long-lived bone marrow plasma cells in humans. Nature *595*, 421-425. 10.1038/s41586-021-03647-4.

189. Turner, J.S., O'Halloran, J.A., Kalaidina, E., Kim, W., Schmitz, A.J., Zhou, J.Q., Lei, T., Thapa, M., Chen, R.E., Case, J.B., Amanat, F., Rauseo, A.M., Haile, A., Xie, X., Klebert, M.K., Suessen, T., Middleton, W.D., Shi, P.Y., Krammer, F., Teefey, S.A., Diamond, M.S., Presti, R.M., and Ellebedy, A.H. (2021). SARS-CoV-2 mRNA vaccines induce persistent human germinal centre responses. Nature *596*, 109-113. 10.1038/s41586-021-03738-2.

190. Whaley, R.E., Ameny, S., Arkatkar, T., Seese, A., Wall, A., Khan, I., Carter, J.J., Scherer, E.M., Rawlings, D.J., Galloway, D.A., McElrath, M.J., Cohen, K.W., and McGuire, A.T. (2021). Generation of a cost-effective cell line for support of high-throughput isolation of primary human B cells and monoclonal neutralizing antibodies. J Immunol Methods *488*, 112901. 10.1016/j.jim.2020.112901.

191. Wieland, A., Patel, M.R., Cardenas, M.A., Eberhardt, C.S., Hudson, W.H., Obeng, R.C., Griffith, C.C., Wang, X., Chen, Z.G., Kissick, H.T., Saba, N.F., and Ahmed, R. (2021). Defining HPV-specific B cell responses in patients with head and neck cancer. Nature *597*, 274-278. 10.1038/s41586-020-2931-3.

192. Yin, Y., Quinlan, B.D., Ou, T., Guo, Y., He, W., and Farzan, M. (2021). In vitro affinity maturation of broader and more-potent variants of the HIV-1-neutralizing antibody CAP256-VRC26.25. Proc Natl Acad Sci U S A *118*. 10.1073/pnas.2106203118.

193. Burton, A.R., Guillaume, S.M., Foster, W.S., Wheatley, A.K., Hill, D.L., Carr, E.J., and Linterman, M.A. (2022). The memory B cell response to influenza vaccination is impaired in older persons. Cell Rep *41*, 111613. 10.1016/j.celrep.2022.111613.

194. Chappert, P., Huetz, F., Espinasse, M.A., Chatonnet, F., Pannetier, L., Da Silva, L., Goetz, C., Megret, J., Sokal, A., Crickx, E., Nemazanyy, I., Jung, V., Guerrera, C., Storck, S., Mahevas, M., Cosma, A., Revy, P., Fest, T., Reynaud, C.A., and Weill, J.C. (2022). Human anti-smallpox long-lived memory B cells are defined by dynamic interactions in the splenic niche and long-lasting germinal center imprinting. Immunity. 10.1016/j.immuni.2022.08.019.

195. Chen, J.S., Chow, R.D., Song, E., Mao, T., Israelow, B., Kamath, K., Bozekowski, J., Haynes, W.A., Filler, R.B., Menasche, B.L., Wei, J., Alfajaro, M.M., Song, W., Peng, L., Carter, L., Weinstein, J.S., Gowthaman, U., Chen, S., Craft, J., Shon, J.C., Iwasaki, A., Wilen, C.B., and Eisenbarth, S.C. (2022). High-affinity, neutralizing antibodies to SARS-CoV-2 can be made without T follicular helper cells. Sci Immunol *7*, eabl5652. 10.1126/sciimmunol.abl5652.

196. Dhanushkodi, N.R., Prakash, S., Srivastava, R., Coulon, P.A., Arellano, D., Kapadia, R.V., Fahim, R., Suzer, B., Jamal, L., Vahed, H., and BenMohamed, L. (2022). Antiviral CD19(+)CD27(+) Memory B Cells Are Associated with Protection from Recurrent Asymptomatic Ocular Herpesvirus Infection. J Virol *96*, e0205721. 10.1128/jvi.02057-21.

197. Dobson, C.S., Reich, A.N., Gaglione, S., Smith, B.E., Kim, E.J., Dong, J., Ronsard, L., Okonkwo, V., Lingwood, D., Dougan, M., Dougan, S.K., and Birnbaum, M.E. (2022). Antigen identification and high-throughput interaction mapping by reprogramming viral entry. Nat Methods *19*, 449-460. 10.1038/s41592-022-01436-z.

198. Gonzales, S.J., Clarke, K.N., Batugedara, G., Garza, R., Braddom, A.E., Reyes, R.A., Ssewanyana, I., Garrison, K.C., Ippolito, G.C., Greenhouse, B., Bol, S., and Bunnik, E.M. (2022). A Molecular Analysis of Memory B Cell and Antibody Responses Against Plasmodium falciparum Merozoite Surface Protein 1 in Children and Adults From Uganda. Front Immunol *13*, 809264. 10.3389/fimmu.2022.809264.

199. Gregoire, C., Spinelli, L., Villazala-Merino, S., Gil, L., Holgado, M.P., Moussa, M., Dong, C., Zarubica, A., Fallet, M., Navarro, J.M., Malissen, B., Milpied, P., and Gaya, M. (2022). Viral infection engenders bona fide and bystander subsets of lung-resident memory

B cells through a permissive mechanism. Immunity *55*, 1216-1233 e1219. 10.1016/j.immuni.2022.06.002.

200. He, T., Zhou, Y., Xu, P., Ling, N., Chen, M., Huang, T., Zhang, B., Yang, Z., Ao, L., Li, H., Chen, Z., Zhang, D., Shi, X., Lei, Y., Wang, Z., Zeng, W., Hu, P., Lan, Y., Zhou, Z., Kang, J., Huang, Y., Shi, T., Pan, Q., Zhu, Q., Ran, X., Zhang, Y., Song, R., Xiang, D., Xiao, S., Zhang, G., Shen, W., Peng, M., Cai, D., and Ren, H. (2022). Safety and antibody response to inactivated COVID-19 vaccine in patients with chronic hepatitis B virus infection. Liver Int *42*, 1287-1296. 10.1111/liv.15173.

201. Hopp, C.S., Skinner, J., Anzick, S.L., Tipton, C.M., Peterson, M.E., Li, S., Doumbo, S., Kayentao, K., Ongoiba, A., Martens, C., Traore, B., and Crompton, P.D. (2022). Atypical B cells up-regulate costimulatory molecules during malaria and secrete antibodies with T follicular helper cell support. Sci Immunol *7*, eabn1250. 10.1126/sciimmunol.abn1250.

202. Hopp, C.S., Taylor, J.J., and Crompton, P.D. (2022). Assessment of Plasmodium falciparum Antigen-Specific B Cells. Methods Mol Biol *2470*, 689-713. 10.1007/978-1-0716-2189-9_52.

203. Imbrechts, M., Maes, W., Ampofo, L., Van den Berghe, N., Calcoen, B., Van Looveren, D., Kerstens, W., Rasulova, M., Vercruysse, T., Noppen, S., Abdelnabi, R., Foo, C., Hollevoet, K., Maes, P., Zhang, X., Jochmans, D., Ven, K., Lammertyn, J., Vanhoorelbeke, K., Callewaert, N., De Munter, P., Schols, D., Thibaut, H.J., Neyts, J., Declerck, P., and Geukens, N. (2022). Potent neutralizing anti-SARS-CoV-2 human antibodies cure infection with SARS-CoV-2 variants in hamster model. iScience *25*, 104705. 10.1016/j.isci.2022.104705.

204. Kim, W., Zhou, J.Q., Horvath, S.C., Schmitz, A.J., Sturtz, A.J., Lei, T., Liu, Z., Kalaidina, E., Thapa, M., Alsoussi, W.B., Haile, A., Klebert, M.K., Suessen, T., Parra-Rodriguez, L., Mudd, P.A., Whelan, S.P.J., Middleton, W.D., Teefey, S.A., Pusic, I., O'Halloran, J.A., Presti, R.M., Turner, J.S., and Ellebedy, A.H. (2022). Germinal centre-driven maturation of B cell response to mRNA vaccination. Nature *604*, 141-145. 10.1038/s41586-022-04527-1.

205. Kraft, J.C., Pham, M.N., Shehata, L., Brinkkemper, M., Boyoglu-Barnum, S., Sprouse, K.R., Walls, A.C., Cheng, S., Murphy, M., Pettie, D., Ahlrichs, M., Sydeman, C., Johnson, M., Blackstone, A., Ellis, D., Ravichandran, R., Fiala, B., Wrenn, S., Miranda, M., Sliepen, K., Brouwer, P.J.M., Antanasijevic, A., Veesler, D., Ward, A.B., Kanekiyo, M., Pepper, M., Sanders, R.W., and King, N.P. (2022). Antigen- and scaffold-specific antibody responses to protein nanoparticle immunogens. Cell Rep Med *3*, 100780. 10.1016/j.xcrm.2022.100780.

206. Kumar, S., Patel, A., Lai, L., Chakravarthy, C., Valanparambil, R., Reddy, E.S., Gottimukkala, K., Davis-Gardner, M.E., Edara, V.V., Linderman, S., Nayak, K., Dixit, K., Sharma, P., Bajpai, P., Singh, V., Frank, F., Cheedarla, N., Verkerke, H.P., Neish, A.S., Roback, J.D., Mantus, G., Goel, P.K., Rahi, M., Davis, C.W., Wrammert, J., Godbole, S., Henry, A.R., Douek, D.C., Suthar, M.S., Ahmed, R., Ortlund, E., Sharma, A., Murali-Krishna, K., and Chandele, A. (2022). Structural insights for neutralization of Omicron variants BA.1, BA.2, BA.4, and BA.5 by a broadly neutralizing SARS-CoV-2 antibody. Science Advances *8*, eadd2032. doi:10.1126/sciadv.add2032.

207. Lederer, K., Bettini, E., Parvathaneni, K., Painter, M.M., Agarwal, D., Lundgreen, K.A., Weirick, M., Muralidharan, K., Castano, D., Goel, R.R., Xu, X., Drapeau, E.M., Gouma, S., Ort, J.T., Awofolaju, M., Greenplate, A.R., Le Coz, C., Romberg, N., Trofe-Clark, J., Malat, G., Jones, L., Rosen, M., Weiskopf, D., Sette, A., Besharatian, B., Kaminiski, M., Hensley, S.E., Bates, P., Wherry, E.J., Naji, A., Bhoj, V., and Locci, M. (2022). Germinal center responses to SARS-CoV-2 mRNA vaccines in healthy and immunocompromised individuals. Cell *185*, 1008-1024 e1015. 10.1016/j.cell.2022.01.027.

208. Lee, J.H., Sutton, H.J., Cottrell, C.A., Phung, I., Ozorowski, G., Sewall, L.M., Nedellec, R., Nakao, C., Silva, M., Richey, S.T., Torre, J.L., Lee, W.H., Georgeson, E., Kubitz, M., Hodges, S., Mullen, T.M., Adachi, Y., Cirelli, K.M., Kaur, A., Allers, C., Fahlberg, M., Grasperge, B.F., Dufour, J.P., Schiro, F., Aye, P.P., Kalyuzhniy, O., Liguori, A., Carnathan, D.G., Silvestri, G., Shen, X., Montefiori, D.C., Veazey, R.S., Ward, A.B., Hangartner, L., Burton, D.R., Irvine, D.J., Schief, W.R., and Crotty, S. (2022). Long-primed germinal centres with enduring affinity maturation and clonal migration. Nature. 10.1038/s41586-022-05216-9.

209. Lee, M.S.J., Inoue, T., Ise, W., Matsuo-Dapaah, J., Wing, J.B., Temizoz, B., Kobiyama, K., Hayashi, T., Patil, A., Sakaguchi, S., Simon, A.K., Bezbradica, J.S., Nagatoishi, S., Tsumoto, K., Inoue, J.I., Akira, S., Kurosaki, T., Ishii, K.J., and Coban, C. (2022). B cell-intrinsic TBK1 is essential for germinal center formation during infection and vaccination in mice. J Exp Med *219*. 10.1084/jem.20211336.

210. Liu, X., Yao, J., Zhao, Y., Wang, J., and Qi, H. (2022). Heterogeneous plasma cells and long-lived subsets in response to immunization, autoantigen and microbiota. Nat Immunol *23*, 1564-1576. 10.1038/s41590-022-01345-5.

211. Newell, K.L., Waldran, M.J., Thomas, S.J., Endy, T.P., and Waickman, A.T. (2022). Simultaneous analysis of antigen-specific B and T cells after SARS-CoV-2 infection and vaccination. Cytometry A *101*, 474-482. 10.1002/cyto.a.24563.

212. Paniskaki, K., Anft, M., Thieme, C.J., Skrzypczyk, S., Konik, M.J., Dolff, S., Westhoff, T.H., Nienen, M., Stittrich, A., Stervbo, U., Witzke, O., Heine, G., Roch, T., and Babel, N. (2022). Severe Acute Respiratory Syndrome Coronavirus 2 Cross-Reactive B and T Cell Responses in Kidney Transplant Patients. Transplant Proc *54*, 1455-1464. 10.1016/j.transproceed.2022.02.016.

213. Pape, K.A., Dileepan, T., Matchett, W.E., Ellwood, C., Stresemann, S., Kabage, A.J., Kozysa, D., Evert, C., Matson, M., Lopez, S., Krueger, P.D., Graiziger, C.T., Vaughn, B.P., Shmidt, E., Rhein, J., Schacker, T.W., Bold, T.D., Langlois, R.A., Khoruts, A., and Jenkins, M.K. (2022). Boosting corrects a memory B cell defect in SARS-CoV-2 mRNA-vaccinated patients with inflammatory bowel disease. JCI Insight *7*. 10.1172/jci.insight.159618.

214. Patel, S.R., Lundgren, T.S., Baldwin, W.H., Cox, C., Parker, E.T., Healey, J.F., Jajosky, R.P., Zerra, P.E., Josephson, C.D., Doering, C.B., Stowell, S.R., and Meeks, S.L. (2022). Neutralizing Antibodies Against Factor VIII Can Occur Through a Non-Germinal Center Pathway. Front Immunol *13*, 880829. 10.3389/fimmu.2022.880829.

215. Rizzuto, G., Brooks, J.F., Tuomivaara, S.T., McIntyre, T.I., Ma, S., Rideaux, D., Zikherman, J., Fisher, S.J., and Erlebacher, A. (2022). Establishment of fetomaternal tolerance through glycan-mediated B cell suppression. Nature *603*, 497-502. 10.1038/s41586-022-04471-0.

216. Rush, S.A., Brar, G., Hsieh, C.L., Chautard, E., Rainho-Tomko, J.N., Slade, C.D., Bricault, C.A., Kume, A., Kearns, J., Groppo, R., Mundle, S.T., Zhang, L., Casimiro, D., Fu, T.M., DiNapoli, J.M., and McLellan, J.S. (2022). Characterization of prefusion-F-specific antibodies elicited by natural infection with human metapneumovirus. Cell Rep *40*, 111399. 10.1016/j.celrep.2022.111399.

217. Salvador, F., Deramoudt, L., Lepretre, F., Figeac, M., Guerrier, T., Boucher, J., Bas, M., Journiac, N., Peters, A., Mars, L.T., and Zephir, H. (2022). A Spontaneous Model of Experimental Autoimmune Encephalomyelitis Provides Evidence of MOG-Specific B Cell Recruitment and Clonal Expansion. Front Immunol *13*, 755900. 10.3389/fimmu.2022.755900.

218. Sangesland, M., Torrents de la Pena, A., Boyoglu-Barnum, S., Ronsard, L., Mohamed, F.A.N., Moreno, T.B., Barnes, R.M., Rohrer,

D., Lonberg, N., Ghebremichael, M., Kanekiyo, M., Ward, A., and Lingwood, D. (2022). Allelic polymorphism controls autoreactivity and vaccine elicitation of human broadly neutralizing antibodies against influenza virus. Immunity. 10.1016/j.immuni.2022.07.006.

219. Schrezenmeier, E., Rincon-Arevalo, H., Jens, A., Stefanski, A.L., Hammett, C., Osmanodja, B., Koch, N., Zukunft, B., Beck, J., Oellerich, M., Pross, V., Stahl, C., Choi, M., Bachmann, F., Liefeldt, L., Glander, P., Schutz, E., Bornemann-Kolatzki, K., Lopez Del Moral, C., Schrezenmeier, H., Ludwig, C., Jahrsdorfer, B., Eckardt, K.U., Lachmann, N., Kotsch, K., Dorner, T., Halleck, F., Sattler, A., and Budde, K. (2022). Temporary antimetabolite treatment hold boosts SARS-CoV-2 vaccination-specific humoral and cellular immunity in kidney transplant recipients. JCI Insight *7*. 10.1172/jci.insight.157836.

220. Tang, J., Zeng, C., Cox, T.M., Li, C., Son, Y.M., Cheon, I.S., Wu, Y., Behl, S., Taylor, J.J., Chakraborty, R., Johnson, A.J., Schiavo, D.N., Utz, J.P., Reisenauer, J.S., Midthun, D.E., Mullon, J.J., Edell, E.S., Alameh, M.G., Borish, L., Teague, W.G., Kaplan, M.H., Weissman, D., Kern, R., Hu, H., Vassallo, R., Liu, S.L., and Sun, J. (2022). Respiratory mucosal immunity against SARS-CoV-2 following mRNA vaccination. Sci Immunol, eadd4853. 10.1126/sciimmunol.add4853.

221. Tarke, A., Coelho, C.H., Zhang, Z., Dan, J.M., Yu, E.D., Methot, N., Bloom, N.I., Goodwin, B., Phillips, E., Mallal, S., Sidney, J., Filaci, G., Weiskopf, D., da Silva Antunes, R., Crotty, S., Grifoni, A., and Sette, A. (2022). SARS-CoV-2 vaccination induces immunological T cell memory able to cross-recognize variants from Alpha to Omicron. Cell *185*, 847-859 e811. 10.1016/j.cell.2022.01.015.

222. Tas, J.M.J., Koo, J.H., Lin, Y.C., Xie, Z., Steichen, J.M., Jackson, A.M., Hauser, B.M., Wang, X., Cottrell, C.A., Torres, J.L., Warner, J.E., Kirsch, K.H., Weldon, S.R., Groschel, B., Nogal, B., Ozorowski, G., Bangaru, S., Phelps, N., Adachi, Y., Eskandarzadeh, S., Kubitz, M., Burton, D.R., Lingwood, D., Schmidt, A.G., Nair, U., Ward, A.B., Schief, W.R., and Batista, F.D. (2022). Antibodies from primary humoral responses modulate the recruitment of naive B cells during secondary responses. Immunity. 10.1016/j.immuni.2022.07.020.

223. Walker, L.M., Shiakolas, A.R., Venkat, R., Liu, Z.A., Wall, S., Raju, N., Pilewski, K.A., Setliff, I., Murji, A.A., Gillespie, R., Makoah, N.A., Kanekiyo, M., Connors, M., Morris, L., and Georgiev, I.S. (2022). High-Throughput B Cell Epitope Determination by Next-Generation Sequencing. Front Immunol *13*, 855772. 10.3389/fimmu.2022.855772.

224. Wang, Z., Muecksch, F., Muenn, F., Cho, A., Zong, S., Raspe, R., Ramos, V., Johnson, B., Ben Tanfous, T., DaSilva, J., Bednarski, E., Guzman-Cardozo, C., Turroja, M., Millard, K.G., Tober-Lau, P., Hillus, D., Yao, K.H., Shimeliovich, I., Dizon, J., Kaczynska, A., Jankovic, M., Gazumyan, A., Oliveira, T.Y., Caskey, M., Bieniasz, P.D., Hatziioannou, T., Kurth, F., Sander, L.E., Nussenzweig, M.C., and Gaebler, C. (2022). Humoral immunity to SARS-CoV-2 elicited by combination COVID-19 vaccination regimens. J Exp Med *219*. 10.1084/jem.20220826.

225. Wang, Z., Zhou, P., Muecksch, F., Cho, A., Ben Tanfous, T., Canis, M., Witte, L., Johnson, B., Raspe, R., Schmidt, F., Bednarski, E., Da Silva, J., Ramos, V., Zong, S., Turroja, M., Millard, K.G., Yao, K.H., Shimeliovich, I., Dizon, J., Kaczynska, A., Jankovic, M., Gazumyan, A., Oliveira, T.Y., Caskey, M., Gaebler, C., Bieniasz, P.D., Hatziioannou, T., and Nussenzweig, M.C. (2022). Memory B cell responses to Omicron subvariants after SARS-CoV-2 mRNA breakthrough infection in humans. J Exp Med *219*. 10.1084/jem.20221006.

226. Weisel, N.M., Joachim, S.M., Smita, S., Callahan, D., Elsner, R.A., Conter, L.J., Chikina, M., Farber, D.L., Weisel, F.J., and Shlomchik, M.J. (2022). Surface phenotypes of naive and memory B cells in mouse and human tissues. Nat Immunol *23*, 135-145. 10.1038/s41590-021-01078-x.

227. Weskamm, L.M., Fathi, A., Raadsen, M.P., Mykytyn, A.Z., Koch, T., Spohn, M., Friedrich, M., Group, M.-M.-S.S., Haagmans, B.L., Becker, S., Sutter, G., Dahlke, C., and Addo, M.M. (2022). Persistence of MERS-CoV-spike-specific B cells and antibodies after late third immunization with the MVA-MERS-S vaccine. Cell Rep Med *3*, 100685. 10.1016/j.xcrm.2022.100685.

228. Zhai, B., Clarke, K., Bauer, D.L., Moehling Geffel, K.K., Kupul, S., Schratz, L.J., Nowalk, M.P., McElroy, A.K., McLachlan, J.B., Zimmerman, R.K., and Alcorn, J.F. (2022). SARS-CoV-2 Antibody Response Is Associated with Age and Body Mass Index in Convalescent Outpatients. J Immunol *208*, 1711-1718. 10.4049/jimmunol.2101156.

229. Zhang, B., Huo, J., Huang, Y., Teo, S.Y., Duan, K., Li, Y., Toh, L.K., Lam, K.P., and Xu, S. (2022). mRNA Booster Vaccination Enhances Antibody Responses against SARS-CoV2 Omicron Variant in Individuals Primed with mRNA or Inactivated Virus Vaccines. Vaccines (Basel) *10*. 10.3390/vaccines10071057.

230. Zhang, Z., Mateus, J., Coelho, C.H., Dan, J.M., Moderbacher, C.R., Galvez, R.I., Cortes, F.H., Grifoni, A., Tarke, A., Chang, J., Escarrega, E.A., Kim, C., Goodwin, B., Bloom, N.I., Frazier, A., Weiskopf, D., Sette, A., and Crotty, S. (2022). Humoral and cellular immune memory to four COVID-19 vaccines. Cell *185*, 2434-2451 e2417. 10.1016/j.cell.2022.05.022.

231. Zhou, C., Osterbye, T., Bach, E., Dahal-Koirala, S., Hoydahl, L.S., Steinsbo, O., Jahnsen, J., Lundin, K.E.A., Buus, S., Sollid, L.M., and Iversen, R. (2022). Focused B cell response to recurring gluten motif with implications for epitope spreading in celiac disease. Cell Rep *41*, 111541. 10.1016/j.celrep.2022.111541.

232. Sokal, A., Bastard, P., Chappert, P., Barba-Spaeth, G., Fourati, S., Vanderberghe, A., Lagouge-Roussey, P., Meyts, I., Gervais, A., Bouvier-Alias, M., Azzaoui, I., Fernandez, I., de la Selle, A., Zhang, Q., Bizien, L., Pellier, I., Linglart, A., Rothenbuhler, A., Marcoux, E., Anxionnat, R., Cheikh, N., Leger, J., Amador-Borrero, B., Fouyssac, F., Menut, V., Goffard, J.C., Storey, C., Demily, C., Mallebranche, C., Troya, J., Pujol, A., Zins, M., Tiberghien, P., Gray, P.E., McNaughton, P., Sullivan, A., Peake, J., Levy, R., Languille, L., Rodiguez-Gallego, C., Boisson, B., Gallien, S., Neven, B., Michel, M., Godeau, B., Abel, L., Rey, F.A., Weill, J.C., Reynaud, C.A., Tangye, S.G., Casanova, J.L., and Mahevas, M. (2023). Human type I IFN deficiency does not impair B cell response to SARS-CoV-2 mRNA vaccination. J Exp Med *220*. 10.1084/jem.20220258.

233. Reed, B.K., Chopp, L.B., Malo, C.S., Renner, D.N., Van Keulen, V.S., Girtman, M.A., Nevala, W.N., Pavelko, K.D., Gil, D., Schrum, A.G., Johnson, A.J., and Pease, L.R. (2015). A Versatile Simple Capture Assay for Assessing the Structural Integrity of MHC Multimer Reagents. PLoS One *10*, e0137984. 10.1371/journal.pone.0137984.

234. Pinto, D., Park, Y.J., Beltramello, M., Walls, A.C., Tortorici, M.A., Bianchi, S., Jaconi, S., Culap, K., Zatta, F., De Marco, A., Peter, A., Guarino, B., Spreafico, R., Cameroni, E., Case, J.B., Chen, R.E., Havenar-Daughton, C., Snell, G., Telenti, A., Virgin, H.W., Lanzavecchia, A., Diamond, M.S., Fink, K., Veesler, D., and Corti, D. (2020). Cross-neutralization of SARS-CoV-2 by a human monoclonal SARS-CoV antibody. Nature *583*, 290-295. 10.1038/s41586-020-2349-y.

235. Seydoux, E., Homad, L.J., MacCamy, A.J., Parks, K.R., Hurlburt, N.K., Jennewein, M.F., Akins, N.R., Stuart, A.B., Wan, Y.H., Feng, J., Whaley, R.E., Singh, S., Boeckh, M., Cohen, K.W., McElrath, M.J., Englund, J.A., Chu, H.Y., Pancera, M., McGuire, A.T., and Stamatatos, L. (2020). Analysis of a SARS-CoV-2-Infected Individual Reveals Development of Potent Neutralizing Antibodies with Limited

Somatic Mutation. Immunity *53*, 98-105 e105. 10.1016/j.immuni.2020.06.001.

236. Wrapp, D., Wang, N., Corbett, K.S., Goldsmith, J.A., Hsieh, C.L., Abiona, O., Graham, B.S., and McLellan, J.S. (2020). Cryo-EM structure of the 2019-nCoV spike in the prefusion conformation. Science *367*, 1260-1263. 10.1126/science.abb2507.

237. Altman, J.D., Moss, P.A., Goulder, P.J., Barouch, D.H., McHeyzer-Williams, M.G., Bell, J.I., McMichael, A.J., and Davis, M.M. (1996). Phenotypic analysis of antigen-specific T lymphocytes. Science *274*, 94-96. 10.1126/science.274.5284.94.

238. Shomuradova, A.S., Vagida, M.S., Sheetikov, S.A., Zornikova, K.V., Kiryukhin, D., Titov, A., Peshkova, I.O., Khmelevskaya, A., Dianov, D.V., Malasheva, M., Shmelev, A., Serdyuk, Y., Bagaev, D.V., Pivnyuk, A., Shcherbinin, D.S., Maleeva, A.V., Shakirova, N.T., Pilunov, A., Malko, D.B., Khamaganova, E.G., Biderman, B., Ivanov, A., Shugay, M., and Efimov, G.A. (2020). SARS-CoV-2 Epitopes Are Recognized by a Public and Diverse Repertoire of Human T Cell Receptors. Immunity *53*, 1245-1257 e1245. 10.1016/j.immuni.2020.11.004.

239. Rodenko, B., Toebes, M., Hadrup, S.R., van Esch, W.J., Molenaar, A.M., Schumacher, T.N., and Ovaa, H. (2006). Generation of peptide-MHC class I complexes through UV-mediated ligand exchange. Nat Protoc *1*, 1120-1132. 10.1038/nprot.2006.121.

240. Bakker, A.H., Hoppes, R., Linnemann, C., Toebes, M., Rodenko, B., Berkers, C.R., Hadrup, S.R., van Esch, W.J., Heemskerk, M.H., Ovaa, H., and Schumacher, T.N. (2008). Conditional MHC class I ligands and peptide exchange technology for the human MHC gene products HLA-A1, -A3, -A11, and -B7. Proc Natl Acad Sci U S A *105*, 3825-3830. 10.1073/pnas.0709717105.

241. Fehlings, M., Chakarov, S., Simoni, Y., Sivasankar, B., Ginhoux, F., and Newell, E.W. (2018). Multiplex peptide-MHC tetramer staining using mass cytometry for deep analysis of the influenza-specific T-cell response in mice. J Immunol Methods *453*, 30-36. 10.1016/j.jim.2017.09.010.

242. Tscharke, D.C., Karupiah, G., Zhou, J., Palmore, T., Irvine, K.R., Haeryfar, S.M., Williams, S., Sidney, J., Sette, A., Bennink, J.R., and Yewdell, J.W. (2005). Identification of poxvirus CD8+ T cell determinants to enable rational design and characterization of smallpox vaccines. J Exp Med *201*, 95-104. 10.1084/jem.20041912.

243. Wu, X., Yang, Z.Y., Li, Y., Hogerkorp, C.M., Schief, W.R., Seaman, M.S., Zhou, T., Schmidt, S.D., Wu, L., Xu, L., Longo, N.S., McKee, K., O'Dell, S., Louder, M.K., Wycuff, D.L., Feng, Y., Nason, M., Doria-Rose, N., Connors, M., Kwong, P.D., Roederer, M., Wyatt, R.T., Nabel, G.J., and Mascola, J.R. (2010). Rational design of envelope identifies broadly neutralizing human monoclonal antibodies to HIV-1. Science *329*, 856-861. 10.1126/science.1187659.

244. McGuire, A.T., Gray, M.D., Dosenovic, P., Gitlin, A.D., Freund, N.T., Petersen, J., Correnti, C., Johnsen, W., Kegel, R., Stuart, A.B., Glenn, J., Seaman, M.S., Schief, W.R., Strong, R.K., Nussenzweig, M.C., and Stamatatos, L. (2016). Specifically modified Env immunogens activate B-cell precursors of broadly neutralizing HIV-1 antibodies in transgenic mice. Nat Commun *7*, 10618. 10.1038/ncomms10618.

245. Garboczi, D.N., Ghosh, P., Utz, U., Fan, Q.R., Biddison, W.E., and Wiley, D.C. (1996). Structure of the complex between human T-cell receptor, viral peptide and HLA-A2. Nature *384*, 134-141. 10.1038/384134a0.